

Aus der Poliklinik für Kieferorthopädie
der Heinrich-Heine-Universität Düsseldorf
Direktor: Univ.-Prof. Dr. med. dent. Dieter Drescher

Stability of Hybrid Hyrax Appliances with
Angle-Stable Mini-Implants
– an In Vitro Study

Dissertation

zur Erlangung des Grades eines Doktors der Zahnmedizin
der Medizinischen Fakultät der Heinrich-Heine-Universität Düsseldorf

vorgelegt von

Geraldine Isabelle Caroline Grützner

2026

Als Inauguraldissertation gedruckt mit Genehmigung der
Medizinischen Fakultät der Heinrich-Heine-Universität Düsseldorf

gez.:

Dekan: Prof. Dr. med. Nikolaj Klöcker

Erstgutachter: Prof. Dr. med. dent. Dieter Drescher

Zweitgutachter: Prof. Dr. med. Dr. med. dent. Jörg Handschel

*Dedicated to my parents
Dres. med. Danuta and Gotthard Grützner*

*“Per Aspera Ad Astra”
- Seneca*

Abstract in German

Hybrid-Hyrax-Apparaturen werden bei Gaumenerweiterungen (RPE) mit skelettaler Verankerung eingesetzt. Diese Studie untersucht Benefit-DIRECT-Mini-Implantate (DG; Direktgruppe) mit winkelstabilen Gewinden (Appliance-First-Workflow) bei maximalen Kräften, die in der Anfangsphase der RPE auftreten. In einem in-vitro Experiment mit 25 Maximalbelastungsversuchen wurden Benefit Standard Mini-Implantate (KG; Kontrollgruppe, PSM Medical Solution) mit Benefit DIRECT Mini-Implantaten (DG; DIRECT Gruppe) verglichen. Die Mini-Implantate, 9 mm lang und 2 mm im Durchmesser, wurden in Kunstknochen (Sawbone, 40 pcf, 15 mm x 10 mm x 10 mm) in einen Schraubstock eingespannt, einer starr, der andere beweglich. In jedem Kunstknochen wurde nach Vorbohrung ein Mini-Implantat mittig inseriert, das andere im Abstand von 8 mm. DG wurden polyaxial in verschiedenen Winkeln 0°, 5°, 10°, 15° Grad (DG0°, DG5°, DG10°, DG15°) durch das Abutment der BMX Expansionsschraube (BMX; PSM Medical Solution) eingesetzt, CG in 0° Winkel und mit Fixationsschraube verbunden. Die Mini-Implantate wurden mit einem elektrischen Schraubendreher (max. 40 Ncm) eingesetzt. Die Dehnschrauben wurden schrittweise aktiviert, bis eine plastische Verformung oder Abkopplung auftrat, wobei die Kräfte elektronisch erfasst wurden. Statistisch signifikante Unterschiede bei den Maximalkräften wurden bezüglich der unterschiedlichen Insertionswinkel bei DG beobachtet. DG war resistenter gegenüber Expansionskräften mit einer durchschnittlichen Maximalkraft von 243 N (DG 0° \bar{x} = 280 ± 44 N; DG 5° \bar{x} = 226 ± 26 N; DG 10° \bar{x} = 226 ± 23 N; DG 15° \bar{x} = 240 ± 29 N) als CG 0° mit \bar{x} = 114 ± 21 N). Signifikante Unterschiede bei den Maximalkräften wurden zwischen DG 0°–15° und CG gefunden, aber nicht zwischen DG 0°–15°. DG zeigte eine höhere Verformungsgrenze als CG (DG 0° \bar{x} = 183 ± 1 N; DG 5° \bar{x} = 183 ± 1 N; DG 10° \bar{x} = 203 ± 8 N; DG 15° \bar{x} = 202 N; CG 0° \bar{x} = 94 ± 2 N). Es gab einen signifikanten Mittelwertsunterschied zwischen DG 10° und DG 15° sowie zwischen DG 0° und DG 5°.

Diese Studie zeigt, dass Mini-Implantat gestützte RPE (MARPE) vor allem bei winkelstabilen Mini-Implantaten wie den DIRECT Vorteile gegenüber herkömmlichen RPE-Verfahren bietet. DG 0° erzielte höhere Maximalkräfte, während DG 10° und DG 15° die höchsten Verformungsgrenzen aufwiesen. Dies spricht für die Nutzung von DIRECT-Mini-Implantaten für MARPE.

Schlüsselwörter: Kieferorthopädie, Mini-Implantate, Hybrid-Hyrax, RPE, MARPE, winkelstabile Implantate; Gaumenerweiterungstechnik; Materialprüfung

Abstract in English

Hybrid hyrax appliances are increasingly used in orthodontics for skeletally and dentally supported rapid palatal expansion (RPE). Mini-implants with matching abutments have to withstand high forces during skeletal expansion. Novel angular-stable mini-implants enable an appliance-first workflow, allowing the appliance to be inserted first, then the mini-implants. The study aimed to compare the load capacity of mini-implants with different coupling types under typical maxillary expansion forces. In an in vitro setup, Benefit Standard mini-implants (CG; control group; PSM Medical Solution) were compared with Benefit DIRECT mini-implants (DG; direct group) comprising a head with an angle-stable thread. Both 9 mm long, 2 mm diameter mini-implants underwent a loading test. Two artificial bones (Sawbone, 40 pcf, 15 mm x 10 mm x 10 mm) were clamped in a vise, one fixed, one movable in one direction. After pre-drilling, a mini-implant was inserted in an artificial bone block using a CAD/CAM printed insertion guide, centered and 8 mm apart, with an electric screwdriver applying a maximum torque of 40 N/cm (NSK iSD900). Benefit DIRECT mini-implants were placed at 0, 5, 10, or 15 degrees (DG 0°, DG 5°, DG 10°, DG 15°) through the corresponding abutments of the BMX expansion screw abutments (Benefit Maxillary Expander, PSM Medical Solution). The control group, Standard Benefit mini-implants, were inserted orthogonally and connected to a BMX with a fixation screw. During 22 BMX activations, forces on the coupling and mini-implants and activation displacement were electronically recorded. Activation stopped upon plastic deformation or decoupling. Statistically significant different maximum forces were observed regarding different insertion angles of DG. DG were more resistant to expansion forces with a total mean maximum force of 243 N (DG 0° \bar{x} = 280 ± 44 N; DG 5° \bar{x} = 226 ± 26 N; DG 10° \bar{x} = 226 ± 23 N; DG 15° \bar{x} = 240 ± 29 N) than CG 0° with \bar{x} = 114 ± 21 N). Significant maximum forces were found between DG 0-15 and CG, but not between DG 0-15. DG yielded a higher mean deformation limit than CG (DG 0° \bar{x} = 183 ± 1 N; DG 5° \bar{x} = 183 ± 1 N; DG 10° \bar{x} = 203 ± 8 N; DG 15° \bar{x} = 202 N; CG 0° \bar{x} = 94 ± 2 N). The mean of DG 10° and DG 15° was significantly different from DG 0° and DG 5°.

This research supports the advantages of mini-implant-assisted RPE (MARPE), especially with angle-stable mini-implants, over traditional RPE. The DG withstood greater forces, with DG 0° tolerating the highest forces, and DG 10° and DG 15° showing the highest deformation. This in vitro study supports the suitability of DIRECT mini-implants for MARPE.

Keywords: orthodontics, mini-implants, hybrid hyrax, RPE, MARPE, angle-stable implants; palatal expansion technique; materials testing

Abbreviations

Alt-RAMEC	Alternate rapid maxillary expansion and constriction (Alt-Ramec)
CG	Control Group Benefit Standard (PSM Medical, Gunningen, Germany)
CG 0°	Control Group Benefit Standard inserted in 0°
DG	Benefit DIRECT Group (PSM Medical, Gunningen, Germany)
DG 0°	Benefit DIRECT inserted in 0 degrees
DG 5°	Benefit DIRECT inserted in 5 degrees
DG 10°	Benefit DIRECT inserted in 10 degrees
DG 15°	Benefit DIRECT inserted in 15 degrees
Pcf	pounds per cubic foot
RPE	Rapid palatal expansion
RME	Rapid maxillary expansion
MARPE	mini-implant-assisted rapid palatal expansion
MPa	Megapascal
MSE	mini-implant-supported maxillary skeletal expansion
n	number
N	Newton
N/cm	Newton/cm
NSK iSD900	NSK screwdriver
SARPE	surgically assisted rapid palatal expansion
SG	surgery guide
BMX	Benefit Maxillary Expander and Benefit Maxillary DIRECT Expander (PSM Medical, Gunningen, Germany)

Table of Contents

1	Introduction	1
1.1	Background.....	1
1.2	Objectives of the Dissertation.....	2
2	Literature.....	3
2.1	Orthodontic Palatal Expansion	3
2.2	Mini-Implant-Assisted Rapid Palatal Expansion.....	3
2.3	Surgically-Assisted Rapid Palatal Expansion.....	4
2.4	Hybrid Hyrax Expansion Appliance.....	4
2.5	Orthodontic Mini-Implant	5
2.6	“DIRECT” Mini-Implant with Polyaxial Thread	6
3	Study Questions.....	8
4	Material and Methods	9
4.1	Orthodontic Mini-Implants and Expansion Screws.....	9
4.2	CAD/CAM Manufactured Insertion Guides.....	14
4.2.1	Design with Blender	14
4.2.2	3D Printing Manufacture with Formlabs	14
4.2.3	Predrilling and Mini-Implant Insertion in Artificial Bone.....	18
4.2.4	Measurement Device	22
4.2.5	Experimental Procedure.....	23
4.3	Statistical Analysis.....	25
5	Results	26
5.1	Results of Descriptive Statistics	26
5.2	Results of Inferential Statistics	31
6	Discussion.....	39
6.1	Discussion of Results.....	39

6.2	Discussion on Angle- and Connection-Dependent Displacement.....	42
6.3	Discussion on Limitations of the Experimental Setup.....	46
6.4	Clinical Conclusion	50
7	References	52
8	Appendix	64
8.1	Figures	64
8.2	Tables.....	65

1 Introduction

1.1 Background

In modern orthodontics palatal expansion is considered the preferred orthodontic procedure for skeletal expansion of the maxilla. It has been used clinically since its first description by Angell in 1860 (Angell, 1860).

Skeletal expansion of the maxilla is indicated in patients with an excessively narrow maxilla, resulting in a crossbite. In the literature, maximum forces of up to 108 N have been reported during the initial phase of palatal expansion (Zimring and Isaacson, 1965). Palatal expansion can be performed using orthodontic appliances with dental anchorage, combined dental and skeletal anchorage (hybrid) (Wilmes et al., 2010), or purely skeletal anchorage (Walter et al., 2023).

Rapid palatal expansion (RPE) is a common orthodontic treatment option combining an orthopedic and dental expansion of the maxilla. During the last decades, mini-implant-assisted rapid palatal expansion (MARPE) as an “adjunct to orthodontic treatment” (Tanaka and Mota-Júnior, 2023) has been widely used to treat maxillary transverse deficiencies in adult patients (Brunetto et al., 2017, Chamberland, 2023) with hybrid hyrax appliances, providing predictable maxillary expansion (Wilmes et al., 2010, Wilmes et al., 2014a, Wilmes et al., 2014b, Othman et al., 2020, Nienkemper et al., 2013b, Feldmann and Bazargani, 2017, Clarenbach et al., 2017). MARPE emerged as a non-surgical alternative to the surgically assisted rapid palatal expansion (SARPE) (de Oliveira et al., 2021).

The generated forces of the hyrax appliance have been studied since 1994. Forces beyond 5 N were categorized as orthopedic forces. They result in substantial anatomical changes in the midface (Shetty et al., 1994, MacGinnis et al., 2014), often positively affecting nasal airflow and resistance (Bazargani et al., 2018).

The hybrid hyrax expansion appliance is characterized by the combination of dental and skeletal anchorage. The forces of the expansion screw positioned centrally in the palate are transmitted to the bone both via the first molars and via the orthodontic mini-implants, which are preferably placed paramedian in the anterior palate in the so-called T zone (Nienkemper et al., 2015, Wilmes et al., 2016, Ludwig et al., 2011, Hourfar et al., 2015a,

Hourfar et al., 2015b). This force distribution can avoid undesirable dental side effects of conventional RPE appliances (Nienkemper et al., 2013b, Wilmes et al., 2014a, Wilmes et al., 2014b) and also produce lower pain levels (Feldmann and Bazargani, 2017).

To perform a palatal expansion using an appliance that is anchored purely skeletally by two mini-implants, the so-called BMX appliance (Benefit Maxillary Expander, PSM Medical Solution, Gunningen, Germany) can be employed. It is also available with four mini-implants (Quadexpander), which is primarily used with adult patients (Wilmes et al., 2021).

The mechanical coupling of mini-implants to appliances can be achieved using adhesive, screwed, or snap-on mechanisms, which are soldered or laser-welded to the expansion screw of an appliance, influencing their load-bearing capacity (de Aguiar et al., 2015, Walter et al., 2013, de la Iglesia et al., 2018).

The market offers various mini-implants in different lengths and diameters, where design significantly impacts primary stability (Wilmes et al., 2008a). Studies indicate that larger diameters support higher loads (Song et al., 2017, Toyoshima and Wakabayashi, 2015, Pimentel et al., 2016, Sfondrini et al., 2018, Chatzigianni et al., 2011, Copello et al., 2021a), while longer implants may reduce mechanical load capacity (Pithon et al., 2013, Tatli et al., 2019). The insertion angle is important for stability and force transmission (Araujo-Monsalvo et al., 2019, Meira et al., 2013, Pickard et al., 2010, Wilmes et al., 2008b). Benefit DIRECT mini-implants, developed by PSM Medical Solutions, incorporate polyaxial, angle-stable threads, accommodating a “misangulation” of up to 15 degrees, and are used in an "appliance first – implants second" workflow (Wilmes, 2022) (p. 3). Despite successful application (Wilmes et al., 2022a), their maximum load capacity remains unidentified.

1.2 Objectives of the Dissertation

This in vitro study aimed to determine the maximum load capacity and elastic deformation threshold of Benefit DIRECT mini-implants inserted at different angles, in comparison to standard Benefit mini-implants, to evaluate their suitability for safely conducting palatal expansion.

2 Literature

2.1 Orthodontic Palatal Expansion

Palatal expansion is generally most effective during early childhood, prior to the pubertal growth spurt, as the palatal suture exhibits the most rapid response to expansion forces. The efficacy of rapid palatal expansion (RPE) in late adolescence and post-pubertal adults remains debated. At this stage, the suture has matured and becomes less receptive to expansion forces, potentially resulting in undesirable dentoalveolar and periodontal soft tissue defects (Copello et al., 2020, Garrett et al., 2008, Greenbaum and Zachrisson, 1982, Kapetanović et al., 2021).

Palatal expansion can be accomplished using the modified Haas appliance. This plastic cap splint is dentally anchored in the maxilla and rests on the mucosa, classified as "tooth-tissue-borne" (Araújo et al., 2020) (p. e923). Transverse effects resemble those produced by maxillary expansion utilizing tooth-borne expansion devices (Hino et al., 2008). Post-puberty, upon completion of growth, transverse maxillary deficiencies can be corrected using mini-implants (Carlson et al., 2016).

2.2 Mini-Implant-Assisted Rapid Palatal Expansion

Since 2010, mini-implant-assisted rapid palatal expansion (MARPE) has become increasingly common in orthodontic therapy with satisfactory outcomes (Wilmes et al., 2010). A recent systematic review and meta-analysis assessing MARPE's effectiveness in transverse skeletal development, dentoalveolar changes, and periodontal effects - across different appliance designs - found that MARPE produces transverse skeletal expansion between 0.31 mm and 2.9 mm, whereas conventional hyrax appliances yield only 0.11 mm to 2.46 mm. The increase in maxillary width with MARPE ranged from 2.89 mm to 9.08 mm, compared to 2.59 mm to 8.51 mm with traditional hyrax appliances (Villa-Obando et al., 2024).

Pure mini-implant-borne skeletal expanders have shown favorable outcomes in research studies. In 2023, Walter et al. examined the load thresholds of various skeletal palatal expansion appliance designs in terms of expansion and torque forces. In their in-vitro study, 30 expanders featuring diverse screw system designs and mini-implant inclinations

were examined, revealing that the loads on appliances with four mini-implants varied from 93 to 166.6 N based on the design, while expanders solely anchored in bone with two mini-implants exhibited lower forces (79.4 N) (Walter et al., 2023).

Breathing improvements resulting from increased nasal and oral inspiratory flow rates, along with decreased patient-reported nasal obstruction, suggest MARPE as an effective non-surgical option for enhancing breathing function in late adolescents and adults with maxillary constriction (Dominguez-Mompell et al., 2025).

2.3 Surgically-Assisted Rapid Palatal Expansion

In older patients, maxillary expansion is often impractical due to common dental complications, leading to the introduction of treatment techniques, such as surgically assisted rapid palatal expansion (SARPE) (Koudstaal et al., 2009, Rachmiel et al., 2020). Maxillary expansion can be accomplished via a non-complete Le Fort I osteotomy without a down fracture, in conjunction with a median palatal osteotomy (Betts et al., 1995, Lin et al., 2023, Mommaerts, 1999).

A study examining the skeletal and dental outcomes of MARPE versus SARPE in post-pubertal adults revealed that MARPE facilitated superior transverse skeletal expansion in the midface and basal maxilla, both anteriorly and posteriorly. In contrast, SARPE caused more buccal tilting of the alveolar process and resulted in V-shaped expansion (de Oliveira et al., 2021). An “asymmetrical expansion of the maxilla” is a common complication following SARPE, often necessitates additional surgery (Lin et al., 2022).

2.4 Hybrid Hyrax Expansion Appliance

The use of mini-implant-assisted rapid palatal expansion (MARPE) in combination with hybrid hyrax appliances (HHE) (Wilmes et al., 2010) or maxillary skeletal expanders (Brunetto et al., 2017, MacGinnis et al., 2014, Wilmes and Drescher, 2008) plays an important role in modern orthodontics. Since 1994, hybrid hyrax appliances and their orthopedic forces (500 g) have been increasingly studied because of their potential to create relevant changes in the craniofacial region. (MacGinnis et al., 2014, Shetty et al., 1994) and on nasal breathing (Bazargani et al., 2018). The hybrid hyrax expansion appliance is characterized by a combination of dental and skeletal anchorage. A

transverse orthodontic expansion screw, placed centrally in the palate, transmits the forces generated during manual expansion to the bone via teeth and mini-implants. Studies recommend insertion of the mini-implants in the anterior palate, in the so-called T-zone, to ensure ideal transmission of forces to the bone (Hourfar et al., 2015a, Hourfar et al., 2015b, Ludwig et al., 2011, Nienkemper et al., 2015, Wilmes et al., 2016). Undesired dental side effects of RPE, for example, in combination with the Alternate rapid maxillary expansion and constriction (Alt-RAMEC) protocol for dental class III treatment (Nienkemper et al., 2013b, Wilmes et al., 2014b, Maino et al., 2023), and associated pain can be reduced by this force distribution (Feldmann and Bazargani, 2017). The Alt-RAMEC protocol consists of alternating weekly cycles of rapid maxillary expansion and constriction to progressively loosen the circummaxillary sutures (Liou and Tsai, 2005). This repeated mechanical stimulus with 1 mm/day expansion and constriction enhances the skeletal response to maxillary protraction (Büyükcavuş, 2019).

2.5 Orthodontic Mini-Implant

The use of mini-implants for orthodontic movements has been common since 1983 because the technique creates stable anchorage conditions (Creekmore and Eklund, 1983). For orthodontic treatment, mini-implants are available in different lengths and their primary stability derives from the thread structure and design of the diameters. mini-implants (Chatzigianni et al., 2011, Nienkemper et al., 2013a, Walter et al., 2013, Wilmes et al., 2008a, Wilmes et al., 2006). Made from biocompatible titanium alloy, orthodontic mini-implants are corrosion-resistant (Gorrieri et al., 2006, Dal Paz et al., 2025), do not lead to an immunological reaction, and are thus widely applicable with a higher success rate compared to stainless steel mini-implants (Mecenas et al., 2020). Some studies demonstrate greater resistance to fractures in mini-implants with larger diameters (Chatzigianni et al., 2011, Copello et al., 2021a, Pimentel et al., 2016, Sadr Haghighi et al., 2019, Sfondrini et al., 2018, Song et al., 2017, Toyoshima and Wakabayashi, 2015).

Certain researchers contend that a greater implant length diminishes mechanical load capacity (Pithon et al., 2013, Tatli et al., 2019). Möhlhenrich (2020) emphasized that implant length plays a significant role in paramedian insertion in the anterior palate

(Möhlhenrich et al., 2020a, Möhlhenrich et al., 2020b). Additionally, Nienkemper proposed that mini-implants measuring 2x9 mm are adequate for achieving stable paramedian stability in the anterior palate (Nienkemper et al., 2015, Nienkemper et al., 2020).

Orthodontic mini-implants in MARPE appliances are mechanically coupled to an expansion screw. They are predominantly connected to abutments through adhesive, screwed or snap-on mechanisms. Studies showed that the connection to the appliance and the design of the mini-implant affect the primary stability and consequently the loading of the mini-implants (Chatzigianni et al., 2011, Copello et al., 2021a, de Aguiar et al., 2015, de la Iglesia et al., 2018, Walter et al., 2013). Various methodological approaches have been developed to quantify fracture rates of orthodontic mini-implants or dental implants. Some authors postulate that fractures are more commonly linked to the connection with the expansion screw and tend to occur more often at the implant neck or abutment region (Assad-Loss et al., 2017, Toyoshima and Wakabayashi, 2015). Conversely, another study found that deformities occur more frequently at the implant shaft (de la Iglesia et al., 2018). Additionally, the insertion angle plays an essential role in the primary stability of the mini-implant and for force transmission to the bone (Araujo-Monsalvo et al., 2019, Meira et al., 2013, Pickard et al., 2010, Wilmes et al., 2008b).

2.6 “DIRECT” Mini-Implant with Polyaxial Thread

Recently, the Benefit DIRECT Mini-Implant (Benefit System; PSM Medical Solutions, Tuttlingen) was developed for orthodontics as an innovation (Wilmes et al., 2022a). Its special polyaxial thread allows the connection to the expansion device through tilting in the grooves of the abutment without the use of an additional mechanical coupling. This design geometry permits the insertion of DIRECT mini-implants at angles between -15 degrees and +15 degrees through the abutments of the expansion screw.

For several years now, screws with a polyaxial, angle-stable thread have been used in orthopedics and trauma surgery for fracture treatment with operative plate osteosynthesis (Liu et al., 2017). They are characterized by a special geometry of the thread at the implant neck, allowing direct tilting with the osteosynthesis plate even when inserted at an angle

(Mendes et al., 2016, Pereira Filho et al., 2013). The literature describes excellent results in orthognathic surgery in the orofacial area for the treatment of sleep apnea (Liu et al., 2017). These aspects make these screw type interesting for orthodontics as well, to enable a more stable connection of orthodontic appliances during MARPE.

In this study, novel Benefit DIRECT mini-implants (Benefit DIRECT, PSM Medical Solutions) were investigated, which were developed for orthodontics based on this principle. With an angle-stable, polyaxial thread at the implant neck, the Benefit DIRECT mini-implants do not require insertion in an exact 90 degrees to the corresponding abutment on the orthodontic hybrid hyrax appliance. Instead they allow a “misangulation” of up to +15 degrees to -15 degrees. This facilitate the insertion of the mini-implants after fitting the expansion device. This method is also called as the "Appliance-First-Implants-Second" workflow. According to Wilmes et al. (2022), by proceeding this way, both the mini-implants and the appliance always fit (Wilmes, 2022).

Several clinical reports on the application of DIRECT mini-implants as anchoring elements to facilitate more effective force transmission in palatal expansion within orthodontics have already demonstrated positive outcomes. Moreover, the simplified insertion procedure of the appliance has been attributed to enhanced patient comfort and increased ease of use for practitioners (Wilmes et al., 2022a). However, the maximum load capacity of these implants is not yet known.

3 Study Questions

To compare the stability of mini-implants inserted at different angles with polyaxial threads and orthogonally inserted mini-implants with screwed connections, the mini-implants were subjected to maximum mechanical loading in vitro. Based on the literature presented, the following null and alternative hypotheses arise:

H0 1 a-c: There is no difference between the perpendicularly inserted Benefit Standard mini-implants and the perpendicular-inserted Benefit DIRECT mini-implants in terms of:

- a. the resistance to maximum force,
- b. the deformation limit, or
- c. the activation until plastic deformation occurs.

H1 1 a-c: There is a difference between the perpendicularly inserted Benefit Standard mini-implants and the perpendicular-inserted Benefit DIRECT mini-implants in terms of:

- a. the resistance to maximum force,
- b. the deformation limit, or
- c. the activation until plastic deformation occurs.

H0 2 a-c: There is no difference between the Benefit DIRECT mini-implants inserted at various angles in terms of:

- a. the maximum force,
- b. the deformation limit, or
- c. the activation.

H1 2 a-c: There is a difference between the Benefit DIRECT mini-implants inserted at various angles implants in terms of:

- a. the maximum force,
- b. the deformation limit, or
- c. the activation.

4 Material and Methods

In this experimental in vitro study, the polyaxially-threaded orthodontic mini-implants inserted at different angles and the orthoradially inserted screw-connected orthodontic mini-implants were analyzed and compared for stability in terms of maximum force, deformation limit, and activation by subjecting the mini-implants to maximum mechanical loading.

4.1 Orthodontic Mini-Implants and Expansion Screws

The study compared two types of Ti6Al4V mini-implants and two types of BMX expansion screws from the Benefit System (PSM Medical, Gunningen, Germany): Benefit Standard mini-implants and Benefit DIRECT mini-implants with a dimension of 2 x 9 mm. The BMX expansion screws (Benefit Maxillary Expander and Benefit Maxillary DIRECT Expander (PSM Medical, Gunningen, Germany)) were spaced 8 mm between the mini-implants and went up to 10 mm expansion. Fig. 1 shows the mini-implants and expansion screws used.

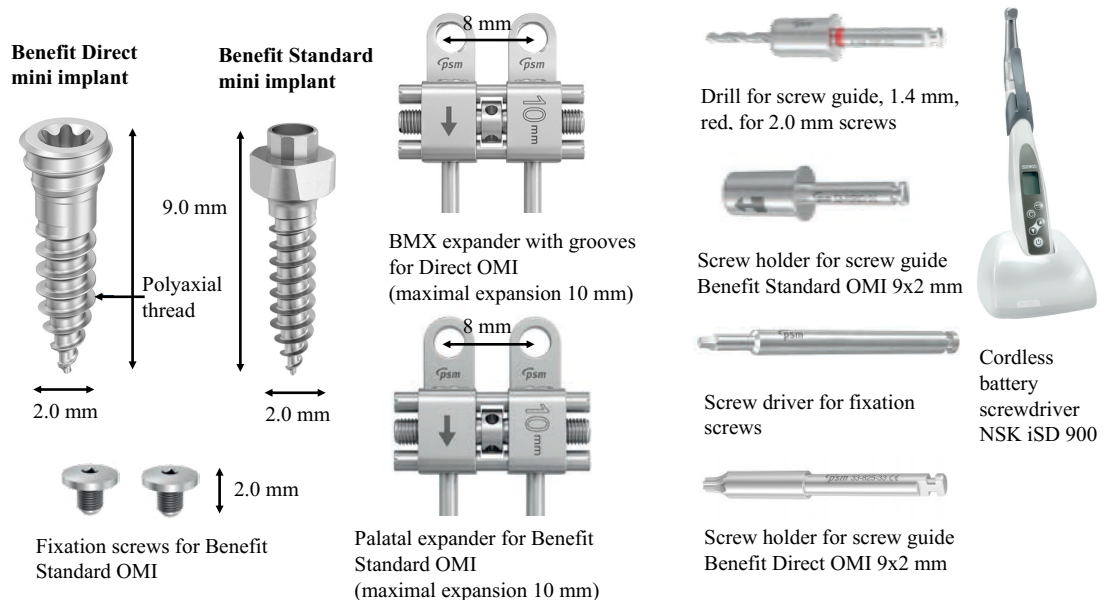


Fig. 1: Material diagram

Benefit DIRECT and Benefit Standard Mini-Implant with the appropriate expansion screws and insertion instruments (PSM Medical) (modified).

Figures 2 and 3 demonstrate two clinical cases of palatal expansion that were achieved through the utilization of a mini-implant-assisted hybrid hyrax appliance (MARPE) in conjunction with hooks for maxillary protraction.

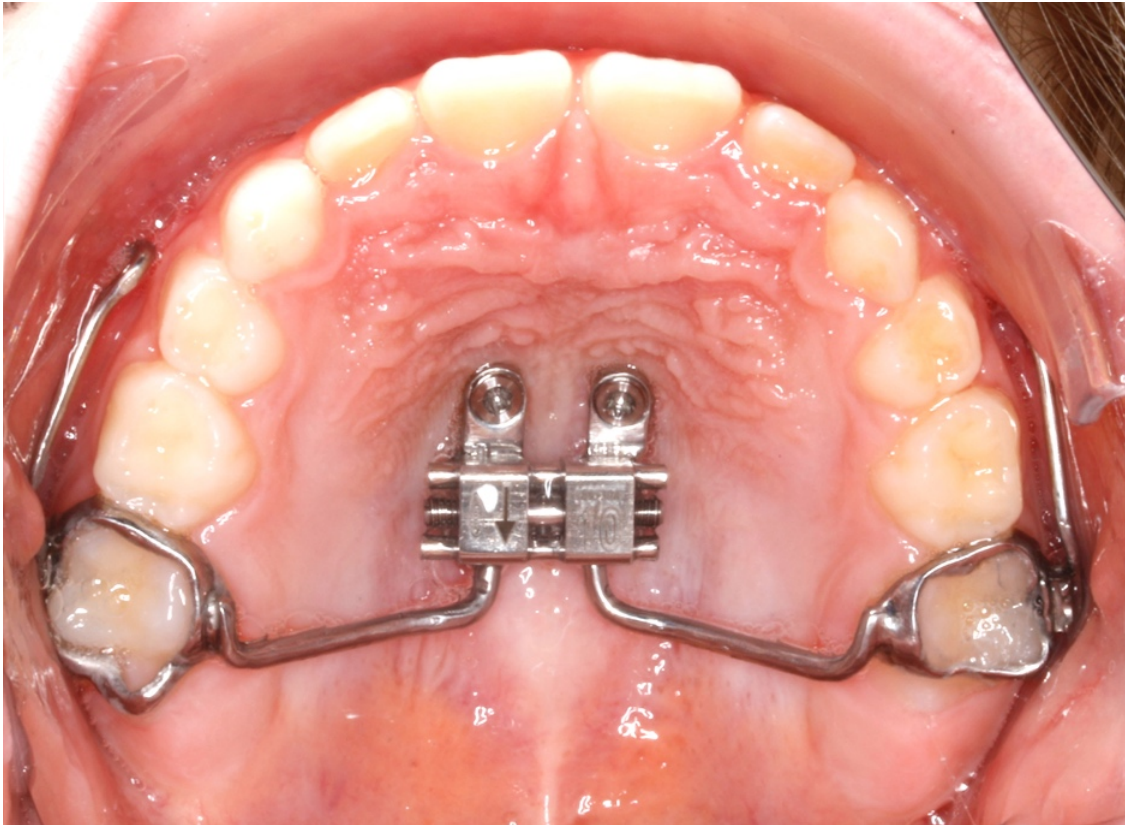


Fig. 2: Clinical example

Hybrid hyrax combined with hooks for maxillary protraction: Hybrid hyrax with DIRECT mini-implants (database photo of Prof. Dr. Drescher).

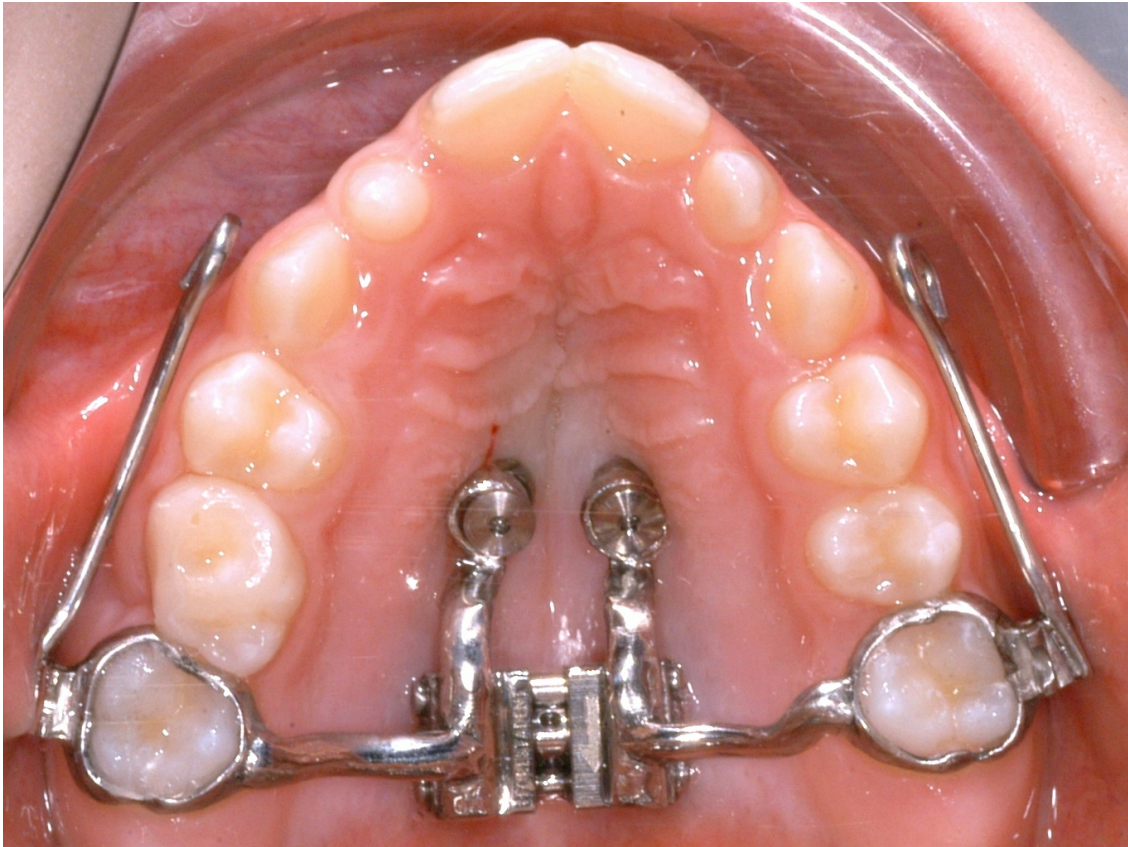


Fig. 3: Clinical example

Hybrid hyrax combined with hooks for maxillary protraction: Standard Benefit mini-implants. (database photo of Prof. Dr. Drescher).

For the control group, two Benefit mini-implants (CG; Control Group) were inserted perpendicularly to the BMX expansion screw abutments utilizing fixation screws. For the other groups, Benefit DIRECT mini-implants were used, distinguished by a polyaxial thread encircling their head. They were screwed directly into the abutment's thread of the BMX DIRECT expansion screw until an insertion torque of 40 N/cm was achieved. Four different angles relative to the perpendicular to the artificial bone were compared (DG; Direct Group; DG 0°, DG 5°, DG 10°, DG 15°) (Fig. 4 and 5).

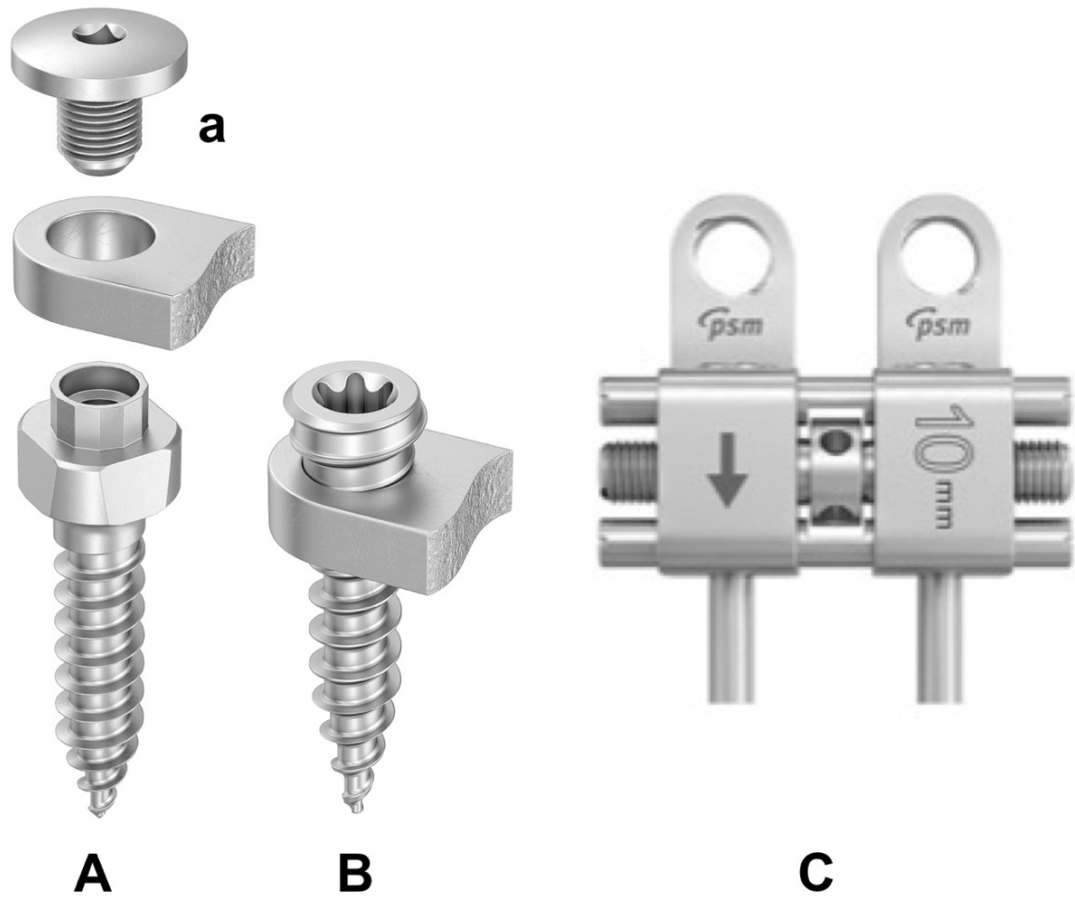


Fig. 4: Two different types of mini-implants and the BMX expansion screw

A: Benefit Standard mini-implant with a: fixation screw; B: DIRECT mini-implant with a polyaxial thread;
 C: BMX palatal expander (PSM Medical) (modified).

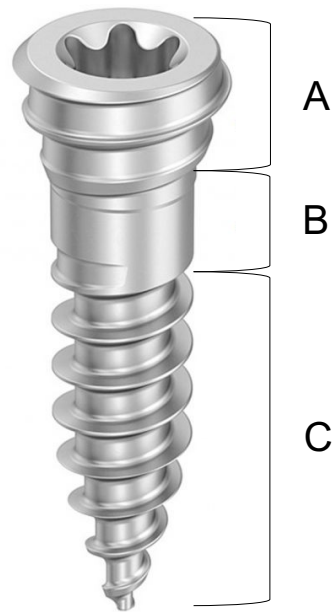


Fig. 5: Benefit direct mini-implant: The polyaxial thread

A: polyaxial thread; B: transmucosal collar; C: intraosseous thread (PSM Medical) (modified).

The sample size of the study was estimated based on the study by Faul et al. 2007 using the program G*Power 3.1 (Faul et al., 2007). The a priori sample size determination (F-test, ANOVA) was calculated with a power of 80%, an alpha error of 5%, and an effect size of $dz=0.8$. Consequently, the analysis required a total sample size of 25. Accordingly, 25 experiments ($n=25$) were performed with two mini-implants each ($n=50$). Table 1 presents the included mini-implants and the summary of the case.

Tab. 1: Summary of the included mini-implants

Included Mini-Implants			
		Value Label	N
Insertion angle	1	Benefit 0°	5
1=CG 0°	2	Direct 0°	5
2=DG 0°	3	Direct 5°	5
3=DG 5°	4	Direct 10°	5
4=DG 10°	5	Direct 15°	5
5=DG 15°			

Included Mini-Implants			
		Value Label	N
mini-implants 1=CG 2=DG	1	Benefit Standard Min- implant 9x2 mm	5
	2	Benefit Direct Mini-implant 9x2 mm	20

4.2 CAD/CAM Manufactured Insertion Guides

4.2.1 Design with Blender

For the precise and reproducible predrilling and insertion of the Benefit and DIRECT mini-implants, two insertion guides were digitally designed for each group using the Blender (Blender Foundation, 2002) program.

4.2.2 3D Printing Manufacture with Formlabs

A total of nine insertion guides were produced using a 3D printer (Formlabs GmbH). First, a support was digitally fabricated as a form-analog matrix to the vise of the experimental setup. This was used for each guide. Each guide was given two sleeves to match either the pilot drill or the insertion instrument.

The Benefit Standard control group received one guide compatible for both predrilling and insertion. The inner diameter of the sleeve was 5 mm and compatible with the pre-drill and insertion instrument, which are both the same size in the Benefit System.

The Benefit DIRECT Groups, DG 0°-15°, each received two guides with angulated sleeves. One guide was used for predrilling and the other for insertion. The inner diameters of the sleeves depended on the pre-drill and insertion instrument; thus, the sleeves for pre-drilling had an inner diameter of 5 mm, and the sleeves for insertion 3 mm. The centers of the implant sleeves were placed at a distance of 5 mm and 13 mm from the edge of the support. The centers of the sleeves were 8 mm apart, based on the selection of the expansion screws (Fig. 6).

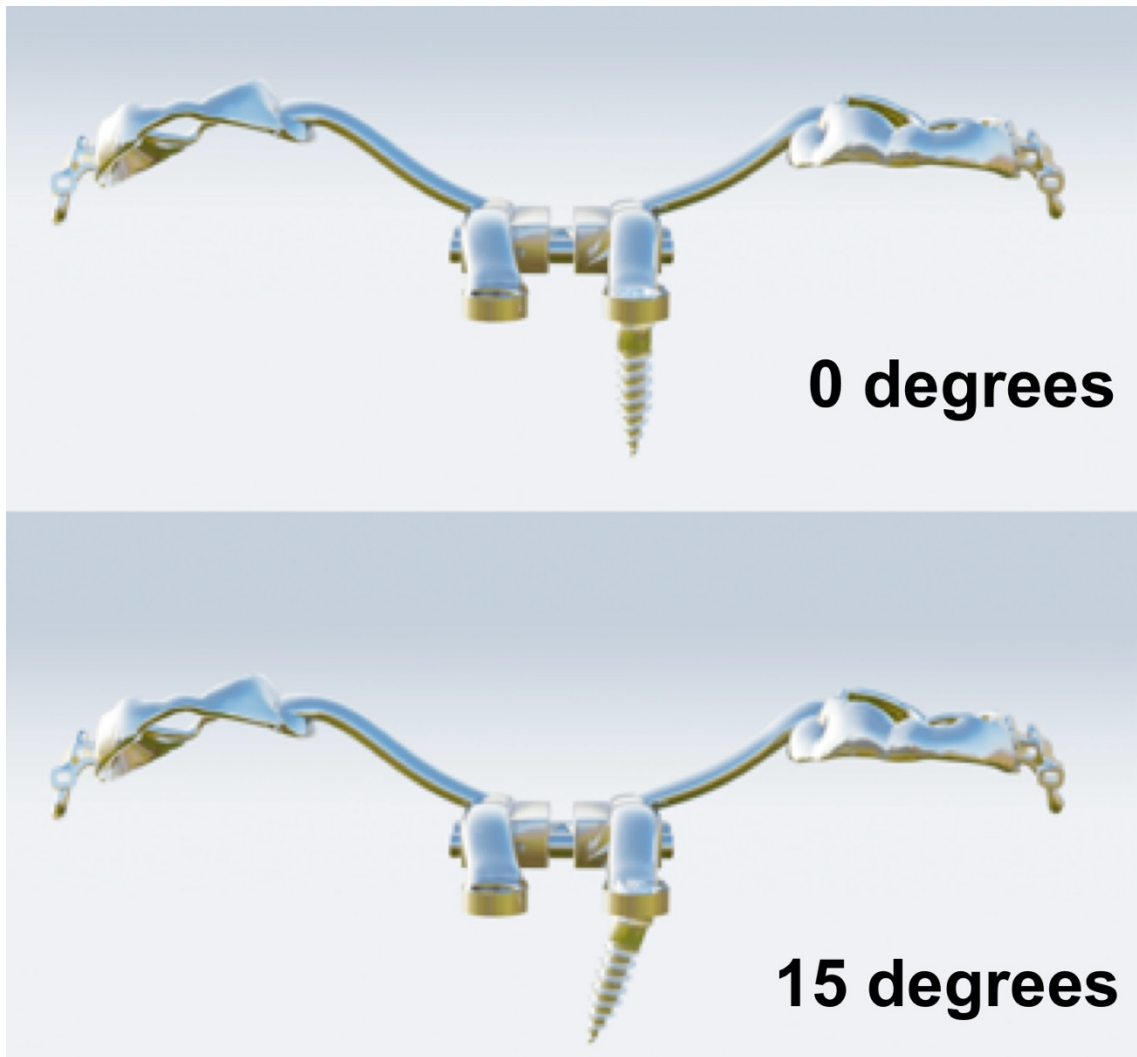


Fig. 6: Example of DIRECT insertion in different angles

upper picture: Hybrid hyrax appliance with Benefit DIRECT mini-implant inserted in 0°; lower picture: Hybrid Hyrax appliance with Benefit DIRECT mini-implant inserted at 15°

After completion in the Blender program (Fig. 7), the digital designs of the double guides were converted into stereolithography (.stl) files and then imported into the PreForm program (Formlabs GmbH). Then, the guides were ideally positioned for the printing process. To create precise printability with few suction cups, mini-raft support structures with a density of 0.9 mm, a contact point size of 0.8 mm to the guide, and a height of 5.00 mm above the raft were generated (Fig. 8 and 9). Figure 8 shows a summary of all the steps before 3D printing (Fig. 10).

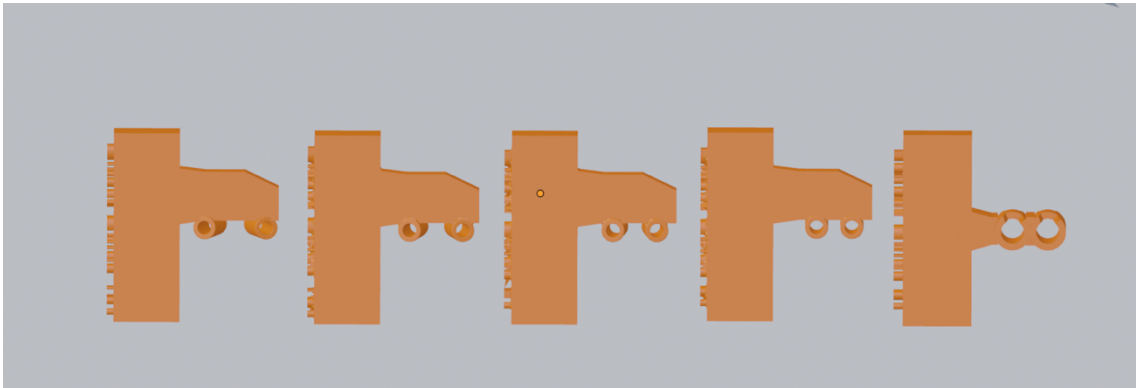


Fig. 7: Computer-assisted fabrication of the insertion guides for predrilling and insertion in Blender
 from left to right; D15°-, D10°-, D5°-, D0°- DIRECT universal guides, B0°-Benefit guide

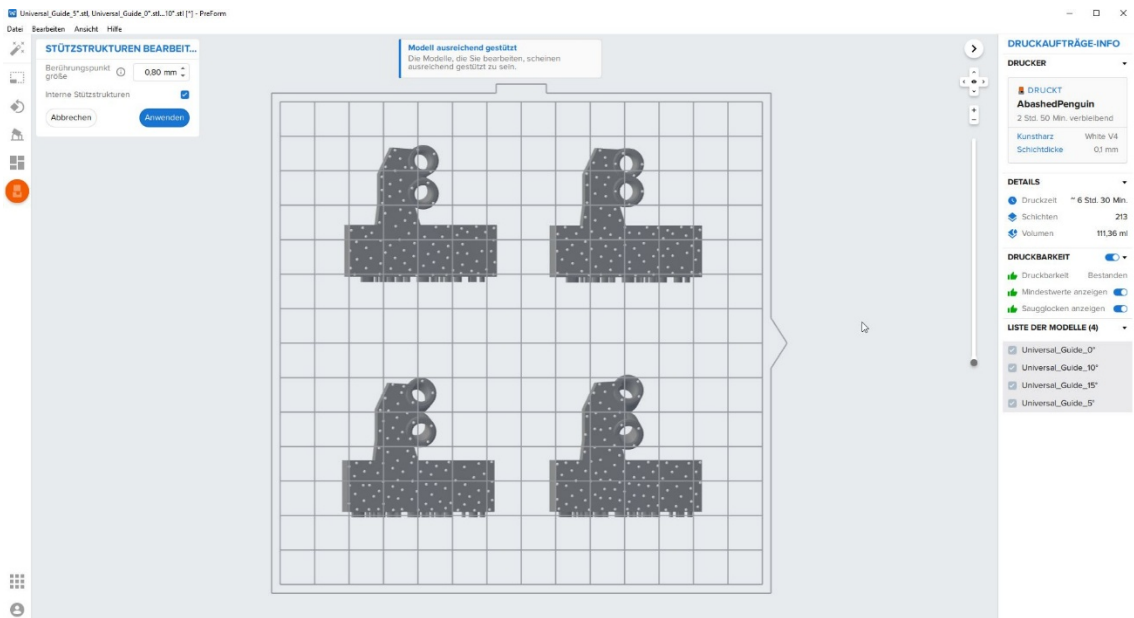


Fig. 8: Double guides with Mini-Raft support structures
 D0°-, D5°-, D10°- and D15°-DIRECT insertion and predrilling (universal) guides ideally positioned for the 3D printing process

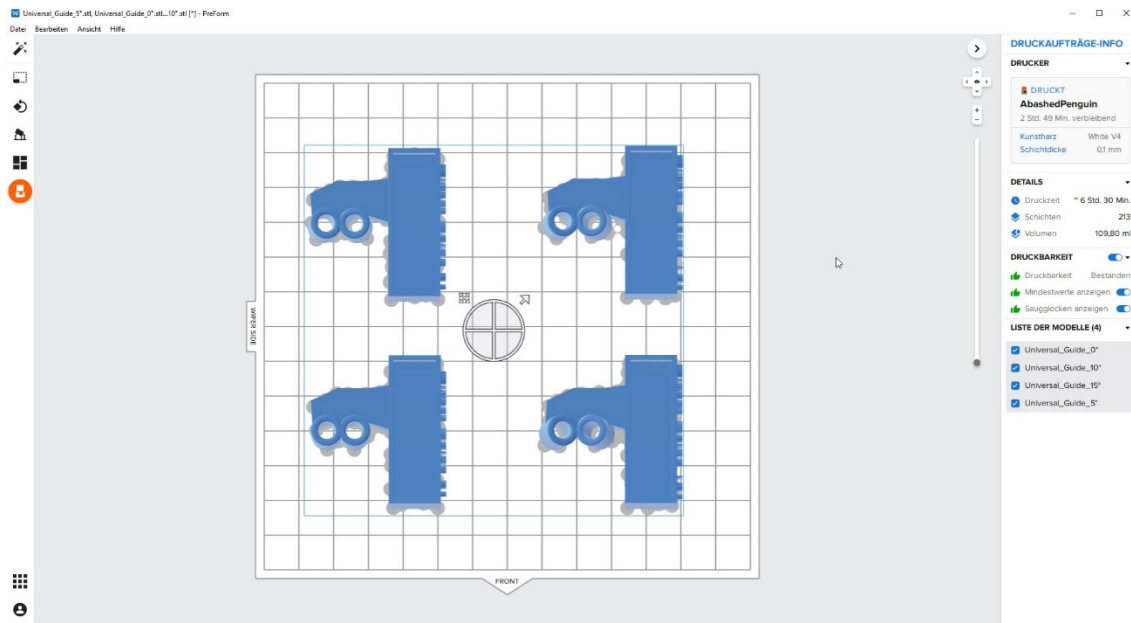


Fig. 9: Double guides position before starting the printing process

D0°, D5°, D10°- and D15°-DIRECT insertion and predrilling (universal) guides ideally positioned for the 3D printing process

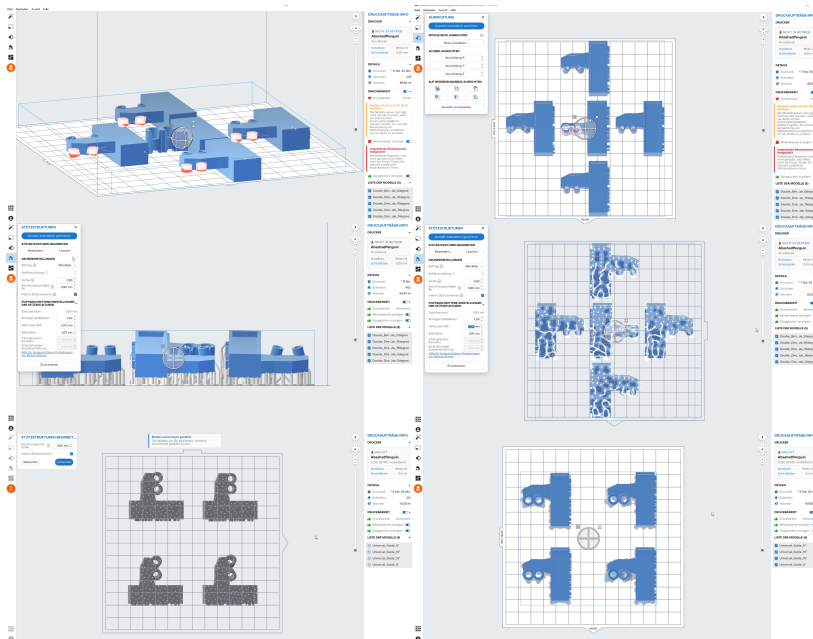


Fig 10: Summary of the preparation of the ideal position for the printing process in Preform
 upper left: imported Double DIRECT Guides (D0°, D5°, D10°, D15°), Benefit Guide 0° in the middle;
 upper right: inclined and elevated position of the guides on the platform; middle left: generated supporting structures; middle right: view on evenly distributed mini-rafts from below; lower left: processed supporting structures; lower right: final position before starting the 3D printing process

For printing, the cartridge and the tray of Dental SG ink were inserted into the Form 2 3D printer (Formlabs GmbH). To prevent the formation of bubbles, the slider was wiped

through the tray, the print surface was inspected, and the 3D printing process was initiated.

Producing a high-resolution 3D print took four and a half hours for five double guides. The process was repeated twice: the first print was for the five double guides intended for the pilot hole, and the second for the four double guides designed for insertion.

Following each print, the Dental SG cartridge was securely locked and removed, and the tray was carefully extracted and closed with the lid. The pressure plate containing the finished double guides was detached and removed using a spatula. The guides, along with support structures, were subsequently immersed in an isopropyl alcohol bath (2-propanol 96%) for thirty minutes. Afterwards, the support structures were carefully removed with a cutter. After drying, the guides were polymerized in a light oven at 60 degrees Celsius for thirty minutes. The guides were then polished at the dental laboratory. Figure 11 presents a summary of the individual steps involved in the CAD/CAM production of the double guides.



Fig. 11: CAD/CAM production steps of the double guides

from left to right: Form 2 3D Printer with printed double Guides; double guides on pressure plate; isopropyl alcohol bath; removing supporting structures with a side cutter; light oven; unpolished double guides from both sides

4.2.3 Predrilling and Mini-Implant Insertion in Artificial Bone

In order to perform reproducible comparisons between the mini-implants, an artificial bone (Sawbone, Malmö, Sweden) was used that is, on average, closest to the human palatal bone. Solid rigid polyurethane foam artificial bone blocks with a density of

40 PCF and a tensile modulus of 1000 MPA, measuring 10 mm long, 10 mm wide, and 15 mm high, were cut to scale specifically for this in vitro study. Table 2 presents the properties of the alternative test medium for human cancellous bone.

Tab. 2: Solid rigid polyurethane foam properties

Density			Compressive		Tensile		Shear	
(PCF)	(g/cc)	Volume Fraction	Strength (Mpa)	Modulus (Mpa)	Strength (Mpa)	Modulus (Mpa)	Strength (Mpa)	Modulus (Mpa)
40	0.64	0.54	31	759	19	1000	11	130

Based on the study by Hosein et al. in which the mini-implants were inserted at a distance of 10 mm from each other in accordance with the American Society for Testing and Materials ASTM (Hosein et al., 2016), the mini-implants were placed next to each other at a distance of 8 mm due to the size of the artificial bone blocks and the prefabricated BMX expansion screws (Benefit Maxillary Expander and Benefit Maxillary DIRECT Expander, PSM Medical Solution). The mini-implants were inserted into artificial bone blocks at the pre-defined angles of 0°, 5°, 10°, or 15° using the CAD/CAM-produced insertion guides. Pre-drilling was performed 6 mm deep for each mini-implant using the individual double guide. The drill guide was then exchanged, and the mini-implants' intraosseous threads were inserted at the different angles through the double guides using an electric screwdriver (NSK iSD900, NSK Europe GmbH, Eschborn, Germany) until an insertion torque of 40 N/cm was reached. The transmucosal collars of both the Benefit Standard and the Benefit DIRECT mini-implants were not inserted into the bone blocks. For gingiva demonstration and standardized stability reasons during the Benefit DIRECT mini-implant insertion, an artificial analog was created using composite rings underneath the DIRECT mini-implants and aluminum pads underneath the BMX expanders during the experiment (Fig. 18), simulating a cantilever arm test (Fig. 12-16).

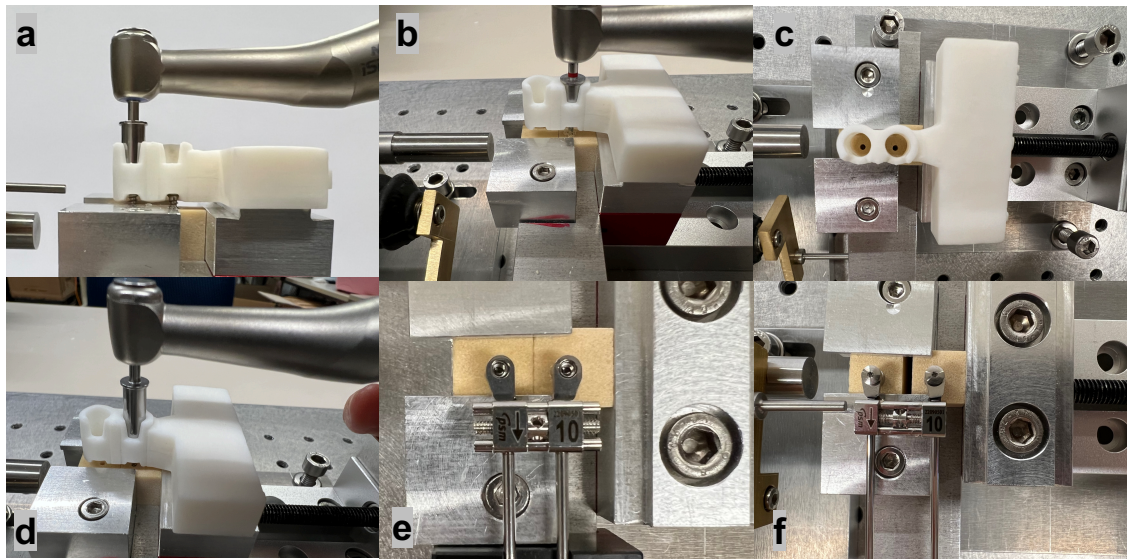


Fig. 12: Benefit standard 0° mini-implant placement

a: Predrilling of the first Benefit Standard mini-implant in 0° with the BENEFIT STANDARD 0° CAD/CAM double guide; b: Predrilling of the second Benefit Standard mini-implant at 0° with the BENEFIT STANDARD 0° CAD/CAM double guide; c: view of the two predrilling holes of 6 mm depth through the BENEFIT STANDARD 0° CAD/CAM double guide; d: insertion of both mini-implants with the BENEFIT STANDARD 0° CAD/CAM double guide; e: view of both inserted mini-implants with the BMX expander on top before the experiment; f: separation of the bone blocks after activation and the end of the experiment with already loosened sensors.

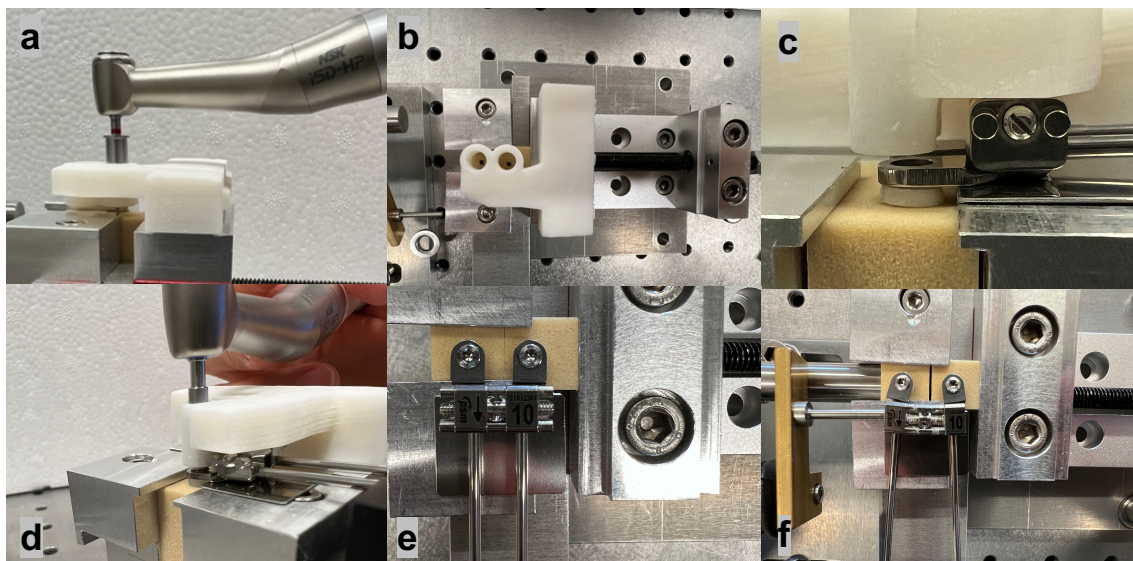


Fig. 13: Benefit direct 0° mini-implant placement

a: Predrilling of both Benefit DIRECT mini-implant holes at 0° with the DIRECT 0° predrilling CAD/CAM double guide; b: view of the two predrilling holes of 6 mm depth through the DIRECT 0° insertion CAD/CAM double guide; c: view from the left side on the DIRECT 0° insertion CAD/CAM double guide, the BMX expander, the 2 mm thick gingiva analog underneath the abutments and the artificial bone blocks; d: insertion of both mini-implants with the DIRECT 0° insertion CAD/CAM double guide through the BMX expander, gingiva analog into the bone blocks; e: view from above of both inserted mini-implants with the BMX expander before the start of the experiment; f: separation of the bone blocks after activation and the end of the experiment with not yet loosened sensors.

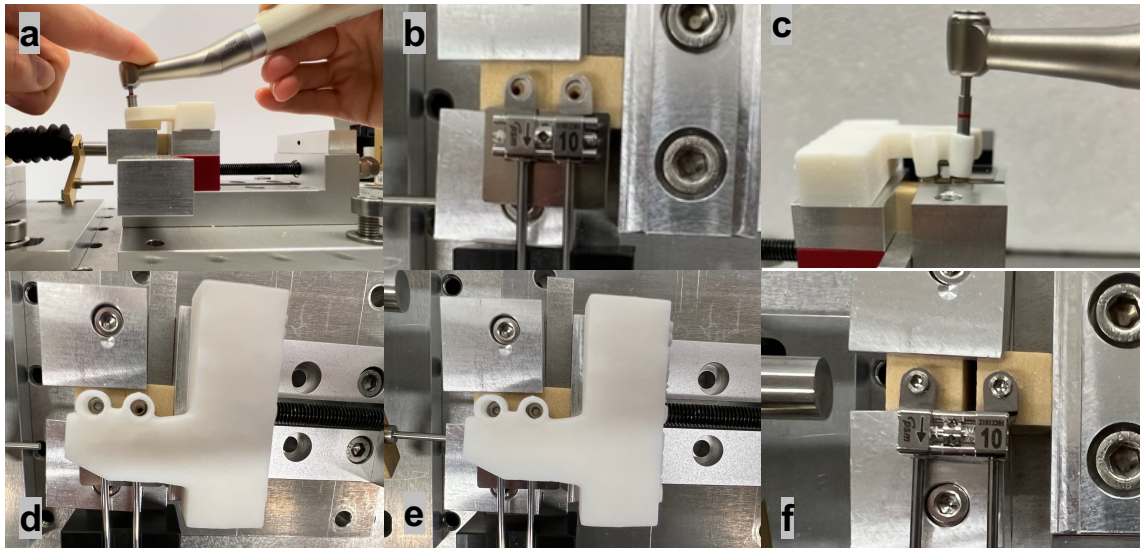


Fig. 14: Benefit direct 5° mini-implant placement

a: Predrilling of both Benefit DIRECT mini-implant holes at 5° and 6 mm depth with the DIRECT 5° predrilling CAD/CAM double guide; b: view of the two predrilling holes, the BMX expander, the 2 mm thick gingiva analog underneath the abutments, the gingiva analog metal plate underneath the BMX and the artificial bone blocks; c: view from the front side of the insertion of the mini-implants at 5° with the DIRECT 5° insertion CAD/CAM double guide; d: view from above after the insertion of the first mini-implant with the DIRECT 5° insertion CAD/CAM double guide through the BMX expander; e: view from above after the insertion of the second mini-implant with the DIRECT 5° insertion CAD/CAM double guide through the BMX expander; f: separation of the bone blocks after activation and the end of the experiment with already loosened sensors.

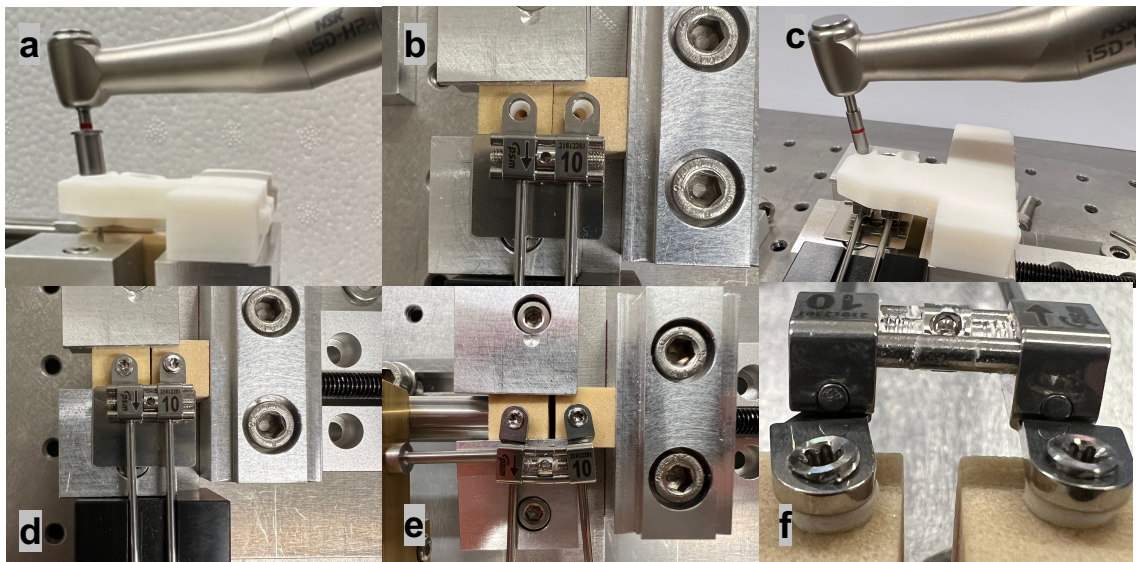


Fig. 15: Benefit direct 10° mini-implant placement

a: Predrilling of both Benefit DIRECT mini-implant holes at 10° and 6 mm depth with the DIRECT 10° predrilling CAD/CAM double guide; b: view of the two predrilling holes, the BMX expander, the 2 mm thick gingiva analog underneath the abutments, the gingiva analog metal plate underneath the BMX, and the artificial bone blocks; c: insertion of the mini-implants at 10° with the DIRECT 10° insertion CAD/CAM double guide; d: view from above after the insertion of both mini-implants through the BMX

expander before the experiment; e: view from above of the separation of the bone blocks and the abutment deformation after the activation and the finished experiment with not yet loosened sensors; f: separation of the bone blocks and abutment deformation after activation and the end of the experiment with already loosened sensors.

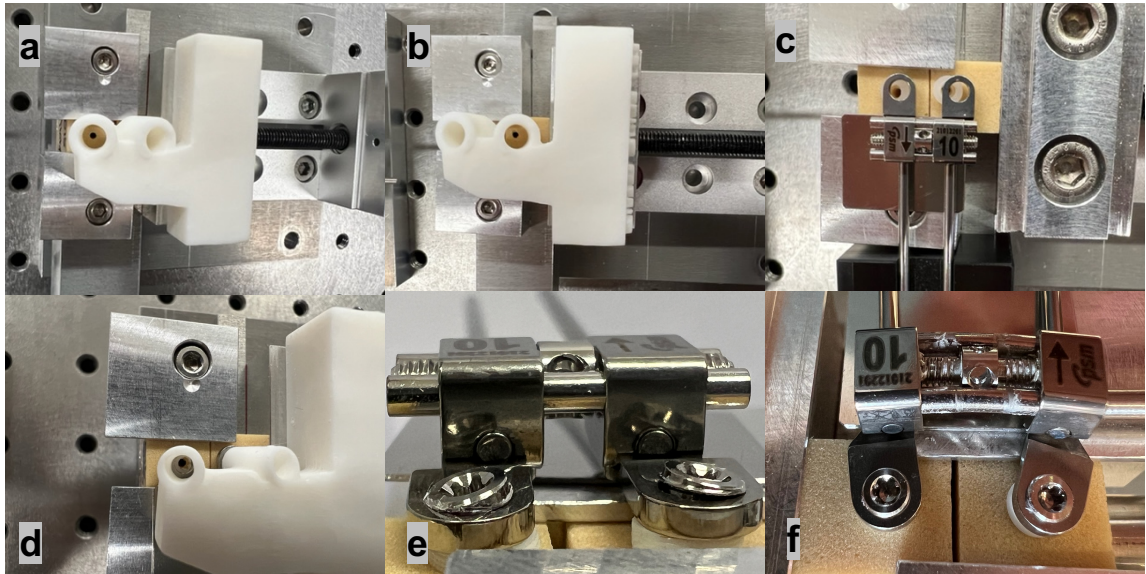


Fig. 16: Benefit direct 15° mini-implant placement

a: Predrilling of the first Benefit DIRECT mini-implant hole at 15° and 6 mm depth with the DIRECT 15° predrilling CAD/CAM double guide; b: view of the second predrilling hole at 15° and 6 mm depth with the DIRECT 15° predrilling CAD/CAM double guide; c: view of both predrilling holes at 15° and 6°mm depth with the BMX expander, the 2 mm thick gingiva analog underneath the abutments, the gingiva analog metal plate underneath the BMX and the artificial bone blocks; d: insertion of the mini-implants at 15° with the DIRECT 15° insertion CAD/CAM double guide; e: view from the front after the insertion of both mini-implants through the BMX expander before the experiment; f: view from above of the separation of the bone blocks and the abutment deformation after the activation and the finished experiment with not yet loosened sensors.

4.2.4 Measurement Device

In a maximum load test, the force acting on the artificial bone as well as its displacement were measured using force and displacement sensors (type 8427; type 8741; Burster *Präzisionsmesstechnik* GmbH und Co. KG, Gernsbach, Germany) mounted in a custom-made apparatus (Fig. 17 and 18). Two artificial blocks were clamped in a vise, one being rigid and fixed, and the other movable in one direction. The contralateral artificial bone blocks were connected to a BMX expansion screw (PSM Medical Solution, Gunningen, Germany).

The tension-compression force sensor (type 8427; Burster *Präzisionsmesstechnik* GmbH und Co. KG) has a measurement range of up to 500 N and was designed on the basis of

a Wheatstone strain gauge bridge, which delivers a stable voltage and provides a nominal characteristic value of 1 mV/V. This force sensor was applied to the movable artificial bone block.

The inductive DC/DC displacement sensor (type 8741; Burster *Präzisionsmesstechnik* GmbH und Co. KG) measured the displacement according to the differential transformer principle (LVDT). The push rod was mounted on ball bearings. The spring pressed the individualized, lateral extension of the probe tip against the BMX expansion screw.

For data acquisition, a universal measurement amplifier (QuantumX, HBM Hottinger, Brüel & Kjær, Darmstadt, Germany) with the associated program MX Assistant version 4.46.6 was used.

4.2.5 Experimental Procedure

Each preparation, including measurement, took 30 minutes. The total activation sequence was one minute or less. Before each trial, the sensors were zeroed, and then the BMX expansion screws were activated. The activations occurred consecutively at a frequency interval of approximately three seconds.

The BMX expansion screws were activated 22 times. The 22 90° activations correspond to an expansion screw opening of 4.4 mm per test. This corresponds to an elongation of 0.8 mm per 360° activation. The experiment was stopped after 22 activations or earlier, as soon as plastic deformation occurred.

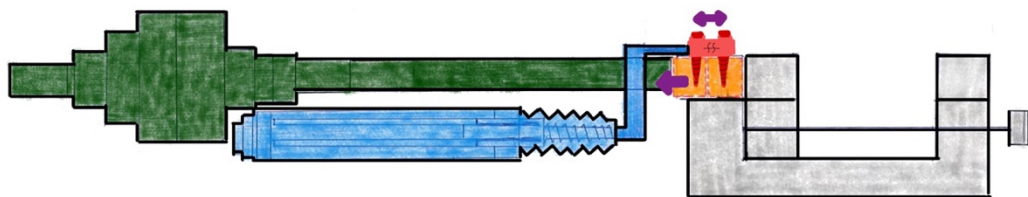


Fig. 17: Schematic illustration of the experimental set-up

green: Force Sensor; blue: Displacement sensor; dark red: mini-implants inserted in bone blocks (orange) and attached to the BMX expander (light red); purple arrows: Direction of activation movement; grey: Vise.

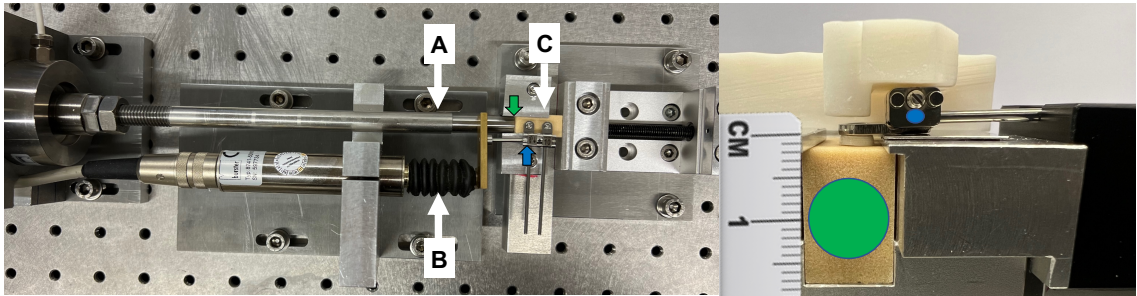


Fig. 18: Picture of the experimental setup

A: force sensor; B: displacement sensor; C: BMX expander with two mini-implants on two sawbones; green arrow and green point: force sensor placement on the artificial bone; blue arrow and blue point: displacement sensor placement on the BMX expander; sensors have been zeroed after the placement before each experiment; ruler: measurement demonstration of the artificial bone and the gingiva replacement in mm.

The force-displacement curves were further processed in Microsoft Excel. For the evaluation of the different stresses in the BMX expansion screw, usual 0.2% limits were defined.

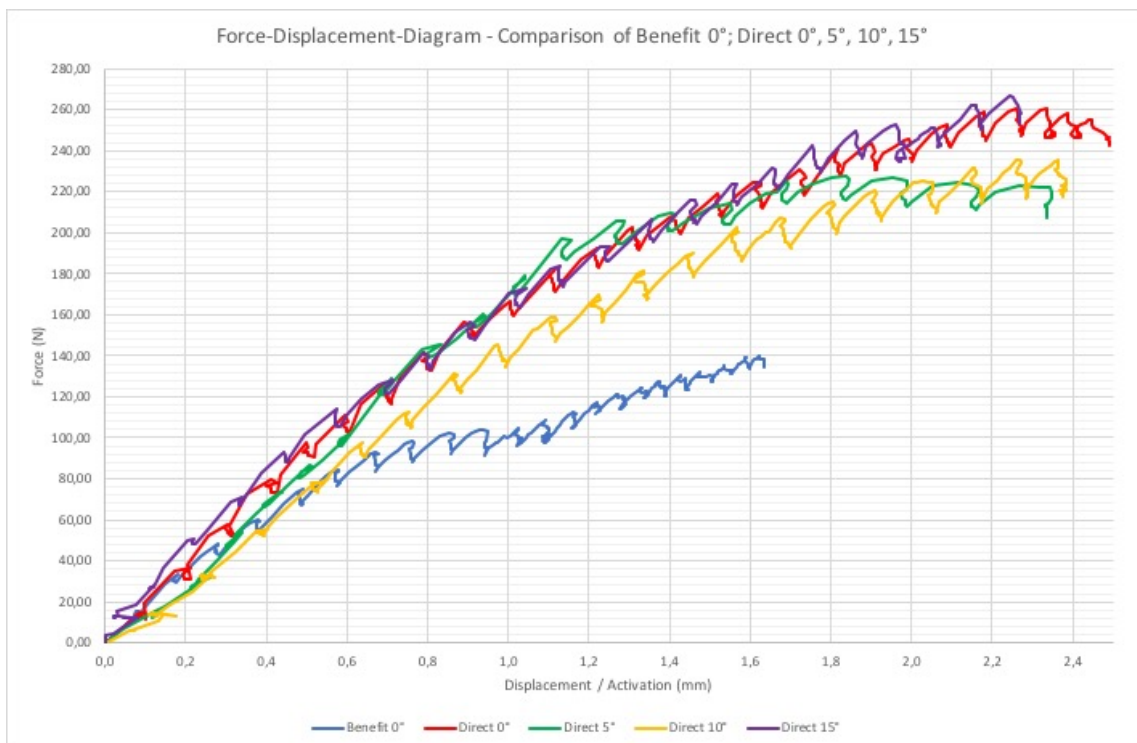


Fig. 19: Force-displacement graph comparing benefit 0°, direct 0°, direct 5°, direct 10° and direct 15°

force-displacement-graph presenting all groups (CG; DGs). The waves in the curves result from the activations of the BMX screws.

4.3 Statistical Analysis

The statistical analyses were conducted in SPSS version 27 (IBM Corp., Armonk, NY, USA). A Kolmogorov-Smirnov and a Shapiro-Wilk test were performed to verify the normal distribution of the variable's maximum forces and deformation limits. In addition to the descriptive statistics, a multivariate ANOVA with post hoc analysis was performed to examine the influence of the angled insertion on the maximum force and the deformation limit. Kruskal-Wallis test with Mann-Whitney U comparisons were applied to determine the differences among the five groups concerning activation. The significance level was set at $p < 0.05$ (Table 3).

Tab. 3: Test of normality

Shapiro Wilk Test				
	Insertion angle	Statistic	df	Sig.
Maximum Force	Benefit 0°	0.868	5	0.258
	Direct 0°	0.881	5	0.316
	Direct 5°	0.991	5	0.982
	Direct 10°	0.901	5	0.417
	Direct 15°	0.833	5	0.146
Deformation Limit	Benefit 0°	0.788	5	0.064
	Direct 0°	0.931	5	0.602
	Direct 5°	0.936	5	0.635
	Direct 10°	0.774	5	0.049
	Direct 15°	0.948	5	0.726
Activation in mm	Benefit 0°	0.782	5	0.058
	Direct 0°	0.844	5	0.177
	Direct 5°	0.653	5	0.003
	Direct 10°	0.873	5	0.280
	Direct 15°	0.864	5	0.242

5 Results

5.1 Results of Descriptive Statistics

To evaluate which mini-implants were able to withstand the highest maximum forces and resisting deformation during palatal expansion and assessing differences in activation length before plastic deformation, a total of 50 mini-implants were tested across 25 measurements. A summary of the groups is given in Table 1. Descriptive data show that DIRECT mini-implants were more resistant to expansion forces, with a total mean maximum force of 243 N, than the control group, with 114 N, implying that the DIRECT mini-implants can withstand higher forces during expansion. The highest mean maximum force was encountered at DG 0° (\bar{x} =280 N \pm 44.2 N), followed by DG 15° (\bar{x} =240 N \pm 29.3 N). DG 5° (\bar{x} =226 N \pm 26.2 N) and DG 10° (\bar{x} =226 N \pm 23.1 N) were similar with a mean maximum force of 226 N (Fig. 20).

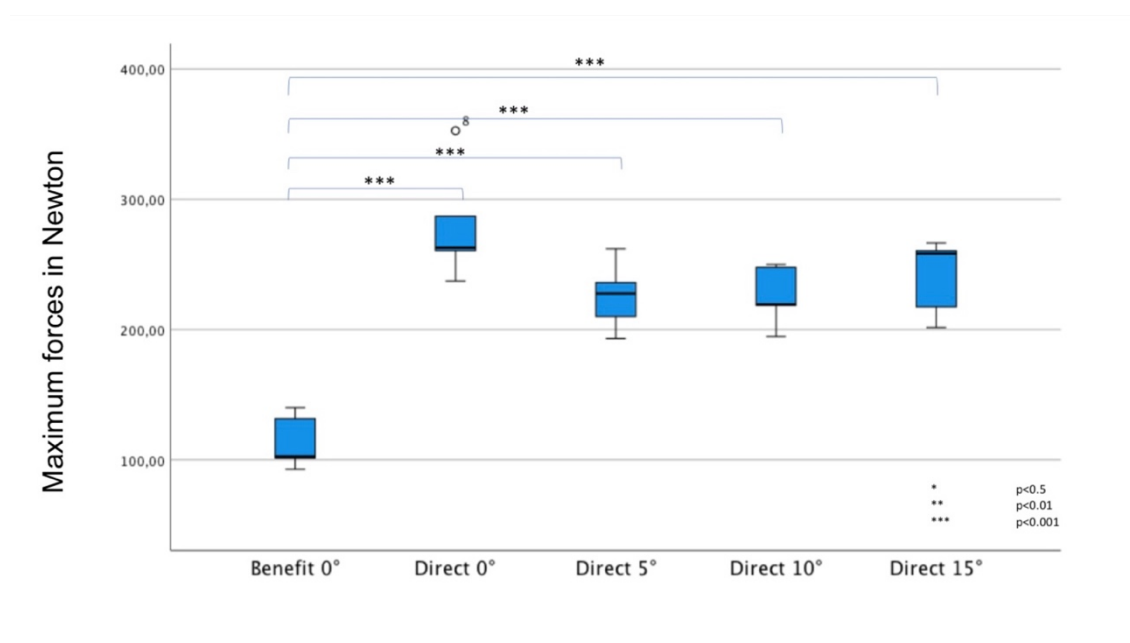


Fig. 20: Maximum forces of all groups

Boxplot shows the significant effect on the maximum forces between the groups ($p < 0.001$).

Regarding the deformation limit, the DIRECT groups were able to withstand higher yield forces (\bar{x} =192 N \pm 10.8 N) until plastic deformation started than the control group (\bar{x} =94 N \pm 2.2 N) (Fig. 21).

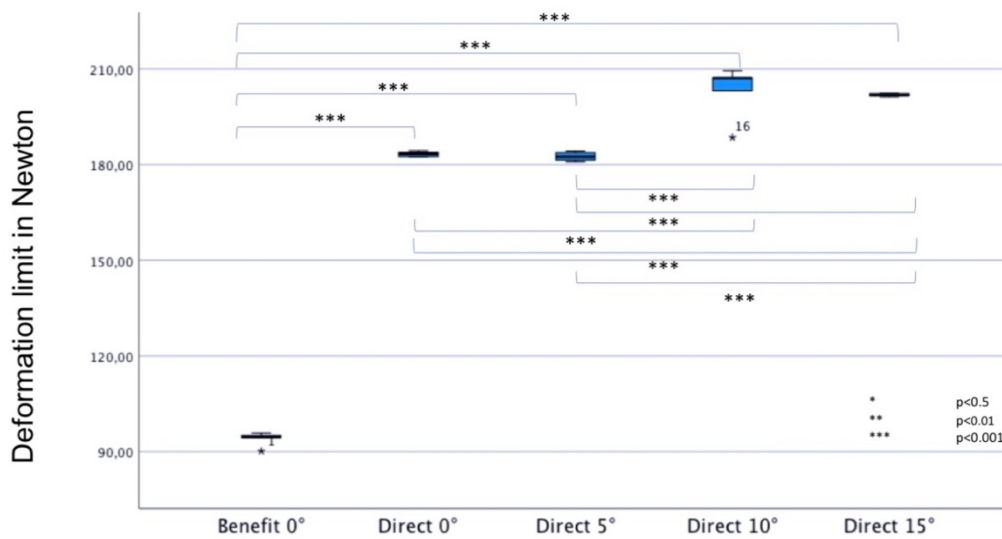


Fig. 21: Deformation limits of all groups

Boxplot shows the significant effect on the deformation limit between the groups ($p < 0.005$).

Consequently, before the onset (0.2%) of plastic deformation, the mean activations in mm of the DIRECT groups were higher ($\bar{x} = 1.3 \text{ mm} \pm 0.3 \text{ mm}$) than those of the control group ($\bar{x} = 0.8 \text{ mm} \pm 0.1 \text{ mm}$) (Tables 4, 5, and 6).

Tab. 4: Descriptive statistics of the maximum force, deformation limit, and activation of all groups

Descriptive Statistics					
Insertion angle 1=Benefit 0° 2=Direct 0° 3=Direct 5° 4=Direct 10° 5=Direct 15°	Mini-Implant Group 1=CG 2=DG		Mean	Std. Deviation	N
Maximum Force in Newton	Benefit 0°	Benefit Standard Mini-implant 9x2 mm	113.7160	20.77782	5
		Total	113.7160	20.77782	5
	Direct 0°	Direct Mini-implant 9x2 mm	280.1120	44.20365	5
		Total	280.1120	44.20365	5
	Direct 5°	Direct Mini-implant 9x2 mm	225.8300	26.15651	5
		Total	225.8300	26.15651	5

Descriptive Statistics						
Insertion angle 1=Benefit 0° 2=Direct 0° 3=Direct 5° 4=Direct 10° 5=Direct 15°	Mini-Implant Group 1=CG 2=DG		Mean	Std. Deviation	N	
	Direct 10°	Direct Mini-implant 9x2 mm	226.0620	23.05593	5	
		Total	226.0620	23.05593	5	
	Direct 15°	Direct Mini-implant 9x2 mm	240.9580	29.34240	5	
		Total	240.9580	29.34240	5	
	Total	Benefit Standard Mini-implant 9x2 mm	113.7160	20.77782	5	
		Direct Miniimplantat 9x2 mm	243.2405	36.94764	20	
		Total	217.3356	62.83931	25	
	Deformation Limit in Newton	Benefit 0°	Benefit Standard Mini-implant 9x2 mm	94.0380	2.22356	5
			Total	94.0380	2.22356	5
Direct 0°		Direct Mini-implant 9x2 mm	183.3400	0.84365	5	
		Total	183.3400	0.84365	5	
Direct 5°		Direct Mini-implant 9x2 mm	182.5800	1.45196	5	
		Total	182.5800	1.45196	5	
Direct 10°		Direct Mini-implant 9x2 mm	203.1460	8.46001	5	
		Total	203.1460	8.46001	5	
Direct 15°		Direct Mini-implant 9x2 mm	201.8860	0.48320	5	
		Total	201.8860	0.48320	5	
Total		Benefit Standard Mini-implant 9x2 mm	94.0380	2.22356	5	
		Direct Mini-implant 9x2 mm	192.7380	10.79985	20	
		Total	172.9980	41.43400	25	
Activation in mm		Benefit 0°	Benefit Standard Mini-implant 9x2 mm	0.8380	0.14584	5
	Total		0.8380	0.14584	5	
	Direct 0°	Direct Mini-implant 9x2 mm	1.1120	0.12755	5	

Descriptive Statistics					
Insertion angle 1=Benefit 0° 2=Direct 0° 3=Direct 5° 4=Direct 10° 5=Direct 15°	Mini-Implant Group 1=CG 2=DG		Mean	Std. Deviation	N
		Total	1.1120	0.12755	5
	Direct 5°	Direct Mini-implant 9x2 mm	1.1620	0.28030	5
		Total	1.1620	0.28030	5
	Direct 10°	Direct Mini-implant 9x2 mm	1.5320	0.40598	5
		Total	1.5320	0.40598	5
	Direct 15°	Direct Mini-implant 9x2 mm	1.2600	0.17321	5
		Total	1.2600	0.17321	5
	Total	Benefit Standard Mini-implant 9x2 mm	0.8380	0.14584	5
		Direct Mini-implant 9x2 mm	1.2665	0.29782	20
		Total	1.1808	0.32306	25

Tab. 5: Estimated marginal means comparing all groups

Marginal Means					
Dependent Variable	Insertion angle 1=Benefit 0° 2=Direct 0° 3=Direct 5° 4=Direct 10° 5=Direct 15°	Mean	Std. Error	95% Confidence Interval	
				Lower Bound	Upper Bound
Maximum Force in Newton	Benefit 0°	113.716	13.360	85.847	141.585
	Direct 0°	280.112	13.360	252.243	307.981
	Direct 5°	225.830	13.360	197.961	253.699
	Direct 10°	226.062	13.360	198.193	253.931
	Direct 15°	240.958	13.360	213.089	268.827
	Benefit 0°	94.038	1.784	90.317	97.759
	Direct 0°	183.340	1.784	179.619	187.061

Marginal Means					
Dependent Variable	Insertion angle 1=Benefit 0° 2=Direct 0° 3=Direct 5° 4=Direct 10° 5=Direct 15°	Mean	Std. Error	95% Confidence Interval	
				Lower Bound	Upper Bound
Deformation Limit in Newton	Direct 5°	182.580	1.784	178.859	186.301
	Direct 10°	203.146	1.784	199.425	206.867
	Direct 15°	201.886	1.784	198.165	205.607
Activation in mm	Benefit 0°	0.838	0.112	0.605	1.071
	Direct 0°	1.112	0.112	0.879	1.345
	Direct 5°	1.162	0.112	0.929	1.395
	Direct 10°	1.532	0.112	1.299	1.765
	Direct 15°	1.260	0.112	1.027	1.493

Tab. 6: Estimated marginal means comparing control group and Direct group

Marginal Means					
Dependent Variable	Mini-implant Group 1=CG 2=DG	Mean	Std. Error	95% Confidence Interval	
				Lower Bound	Upper Bound
Maximum Force in Newton	Benefit Standard Mini-implant	113.716	13.360	85.847	141.585
	Direct Mini-implant	243.241	6.680	229.306	257.175
Deformation Limit in Newton	Benefit Standard Mini-implant	94.038	1.784	90.317	97.759
	Direct Mini-implantat	192.738	0.892	190.877	194.599

Marginal Means					
Dependent Variable	Mini-implant Group 1=CG 2=DG	Mean	Std. Error	95% Confidence Interval	
				Lower Bound	Upper Bound
Activation in mm	Benefit Standard Mini-implant	0.838	0.112	0.605	1.071
	Direct Mini-implant	1.267	0.056	1.150	1.383

5.2 Results of Inferential Statistics

ANOVA demonstrated a significant effect of angle-altered insertion on the maximum forces and deformation limits ($F(8, 40) = 15.3, p < 0.001$, Pillai's Trace = 1.51). The result of Box's test was significant ($p < 0.001$), and the Levene's test based on means showed equality (Tables 7, 8, and 9).

Tab. 7: Box's Test

Box's Test of Equality of Covariance Matrices	
Box's M	47.667
F	3.095
df1	12
df2	2964.706
Sig.	<0.001

Tab. 8: Levene's test

Levene's Test of Equality of Error Variances					
		F	df1	df2	Sig.
Maximum Force	Based on Mean	0.792	4	20	0.544
Deformation Limit	Based on Mean	3.949	4	20	0.016

Tab. 9: Multivariate ANOVA

Multivariate Tests							
Effect		Value	F	Hypothesis df	Error df	Sig.	Partial Eta Squared
Intercept	Pillai's Trace	1.000	22894.101	2.000	19.000	<0.001	1.000
Angle	Pillai's Trace	1.507	15.298	8.000	40.000	<0.001	0.754

At a Bonferroni-corrected alpha error level of .025, subsequent ANOVA for maximum forces and deformation limits each showed a significant effect: maximum force $F(4, 20)=21.55$, $p<0.001$; deformation limit $F(4, 20)=642.28$, $p<0.001$ (Tables 10 and 11).

Tab. 10: ANOVA

ANOVA							
Insertion angle 1=Benefit 0° 2=Direct 0° 3=Direct 5° 4=Direct 10° 5=Direct 15°			Sum of Squares	df	Mean Square	F	Sig.
Maximum Force	Between (Combined) Groups		76921.103	4	19230.276	21.547	0.000
	Within Groups		17849.584	20	892.479		
	Total		94770.687	24			
Deformation Limit	Between (Combined) Groups		40884.359	4	10221.090	642.275	0.000

ANOVA						
Insertion angle 1=Benefit 0° 2=Direct 0° 3=Direct 5° 4=Direct 10° 5=Direct 15°		Sum of Squares	df	Mean Square	F	Sig.
	Within Groups	318.278	20	15.914		
	Total	41202.637	24			

Tab. 11: ANOVA measures of association

Measures of Association		
Insertion angle 1=Benefit 0°, 2=Direct 0°, 3=Direct 5°, 4=Direct 10°, 5=Direct 15°	Eta	Eta Squared
Maximum Force	0.901	0.812
Deformation Limit	0.996	0.992

Bonferroni post hoc tests revealed that DIRECT mini-implants had a significantly higher maximum force than Benefit mini-implants, regardless of the angle of insertion: DG 0° (D=-166.4, p<0.001); DG 5° (D=-112.11, p<0.001); DG 10° (D=-112.35, p<0.001); DG 15° (D=-127.24, p<0.001). There were no significant mean differences between the DIRECT groups DG 0°-15°.

Moreover, Bonferroni post hoc tests showed that all four angles (0°, 5°, 10°, 15°) of the DIRECT groups resulted in a significant increase in the deformation limit compared to the control group; DG 0° (D=-89.3, p<0.001); DG 5° (D=-88.54, p<0.001); DG 10° (D=-109.11, p<0.001); DG 15° (D=-107.85, p<0.001). Furthermore, the DG 10° (D=-19.81, p<0.001) and DG 15° (D=-18.55, p<0.001) had a significant mean difference compared to the DG 0°. In addition, DG 10° (D=-20.57, p<0.001) and DG 15° (D=-19.31, p<0.001) had a significant mean difference compared to DG 5°. Differences could not be detected between the DG 0° and DG 5° or between the DG 10° and DG 15° (Table 12).

Tab. 12: Bonferroni post hoc test comparing all groups for maximum force and deformation limit

Multiple Comparisons							
Bonferroni							
Dependent Variable	Insertion angle 1=Benefit 0°, 2=Direct 0°, 3=Direct 5°, 4=Direct 10°, 5=Direct 15°		Mean Difference (I-J)	Std. Error	Sig.	95% Confidence Interval	
	Lower Bound	Upper Bound					
Maximum Force	Benefit 0°	Direct 0°	-166.396	18.894	<0.001	-225.977	-106.815
		Direct 5°	-112.114	18.894	<0.001	-171.695	-52.533
		Direct 10°	-112.346	18.894	<0.001	-171.927	-52.765
		Direct 15°	-127.242	18.894	<0.001	-186.823	-67.661
	Direct 0°	Benefit 0°	166.396	18.894	<0.001	106.815	225.977
		Direct 5°	54.282	18.894	0.094	-5.299	113.863
		Direct 10°	54.050	18.894	0.097	-5.531	113.631
		Direct 15°	39.154	18.894	0.514	-20.427	98.735
	Direct 5°	Benefit 0°	112.114	18.894	<0.001	52.533	171.695
		Direct 0°	-54.282	18.894	0.094	-113.863	5.299
		Direct 10°	-0.232	18.894	1.000	-59.813	59.349
		Direct 15°	-15.128	18.894	1.000	-74.709	44.453
	Direct 10°	Benefit 0°	112.346	18.894	<0.001	52.765	171.927
		Direct 0°	-54.050	18.894	0.097	-113.631	5.531
		Direct 5°	0.232	18.894	1.000	-59.349	59.813
		Direct 15°	-14.896	18.894	1.000	-74.477	44.685
	Direct 15°	Benefit 0°	127.242	18.894	<0.001	67.661	186.823
		Direct 0°	-39.154	18.894	0.514	-98.735	20.427

Multiple Comparisons							
Bonferroni							
Dependent Variable	Insertion angle 1=Benefit 0°, 2=Direct 0°, 3=Direct 5°, 4=Direct 10°, 5=Direct 15°	Mean Difference (I-J)	Std. Error	Sig.	95% Confidence Interval		
					Lower Bound	Upper Bound	
	Direct 5°	15.128	18.894	1.000	-44.453	74.709	
	Direct 10°	14.896	18.894	1.000	-44.685	74.477	
Deformation Limit	Benefit 0°	Direct 0°	-89.302	2.523	<0.001	-97.258	-81.346
		Direct 5°	-88.542	2.523	<0.001	-96.498	-80.586
		Direct 10°	-109.108	2.523	<0.001	-117.064	-101.152
		Direct 15°	-107.848	2.523	<0.001	-115.804	-99.892
	Direct 0°	Benefit 0°	89.302	2.523	<0.001	81.346	97.258
		Direct 5°	0.760	2.523	1.000	-7.196	8.716
		Direct 10°	-19.806	2.523	<0.001	-27.762	-11.850
		Direct 15°	-18.546	2.523	<0.001	-26.502	-10.590
	Direct 5°	Benefit 0°	88.542	2.523	<0.001	80.586	96.498
		Direct 0°	-0.760	2.523	1.000	-8.716	7.196
		Direct 10°	-20.566	2.523	<0.001	-28.522	-12.610
		Direct 15°	-19.306	2.523	<0.001	-27.262	-11.350
	Direct 10°	Benefit 0°	109.108	2.523	<0.001	101.152	117.064
		Direct 0°	19.806	2.523	<0.001	11.850	27.762
		Direct 5°	20.566	2.523	<0.001	12.610	28.522
		Direct 15°	1.260	2.523	1.000	-6.696	9.216
Direct 15°	Benefit 0°	107.848	2.523	<0.001	99.892	115.804	

Multiple Comparisons						
Bonferroni						
Dependent Variable	Insertion angle 1=Benefit 0°, 2=Direct 0°, 3=Direct 5°, 4=Direct 10°, 5=Direct 15°	Mean Difference (I-J)	Std. Error	Sig.	95% Confidence Interval	
					Lower Bound	Upper Bound
	Direct 0°	18.546	2.523	<0.001	10.590	26.502
	Direct 5°	19.306	2.523	<0.001	11.350	27.262
	Direct 10°	-1.260	2.523	1.000	-9.216	6.696

Because of the non-normal distribution of data regarding the variable activation in mm, the evaluation was conducted by non-parametric tests. An independent-samples Kruskal-Wallis test showed that the distribution of activation in mm is not the same across the DIRECT groups and the control group; $\chi^2(1)=8.747$; $p=0.003$ (Tables 13 and 14).

Tab. 13: Non-parametric test summary for the activation in mm between the control group and Direct groups

Hypothesis Test Summary				
	Null Hypothesis	Test	Sig.	Decision
1	The distribution of Activation in mm is the same across categories of mini-implant group 1=CG 2=DG	Independent-Samples Mann-Whitney U Test	0.001	Reject the null hypothesis.
2	The distribution of Activation in mm is the same across categories of mini-implant group 1=CG 2=DG	Independent-Samples Kruskal-Wallis Test	0.003	Reject the null hypothesis.

Tab. 14: Kruskal-Wallis Test for the activation across the control group and all Direct groups

Independent-Samples Kruskal-Wallis Test Summary	
Total N	25
Test Statistic	8.747
Degree Of Freedom	1
Asymptotic Sig.(2-sided test)	0.003

Likewise, an independent-samples Kruskal-Wallis test demonstrated that the distribution of activation in mm was influenced by the insertion angle; $\text{Chi}^2(4)=13.808$; $p=0.008$. (Table 15)

Tab. 15: Kruskal-Wallis Test for activation across the control group and the angle-altered Direct groups 1-4

Independent-Samples Kruskal-Wallis Test Summary	
Total N	25
Test Statistic	13.808
Degree Of Freedom	4
Asymptotic Sig.(2-sided test)	0.008

Post hoc tests, according to Dunn-Bonferroni, only revealed a significant difference in activation in millimeters between the control group and the DIRECT DG 10°; $z = -3.526$; Asymp.Sig. (2-tailed) = 0.004), assuming that an angle-altered insertion has the desired effect of increasing activation during palatal expansion before plastic deformation. According to Cohen (1992), this is a strong effect, with a correlation coefficient of $r = 1.1$ (Table 16).

Tab. 16: Post hoc Dunn-Bonferroni test after Kruskal-Wallis test

Pairwise Comparisons of Insertionangle					
1=CG 0°, 2=DG 0°, 3=DG 5°, 4=DG 10°, 5=DG 15°					
Sample 1-Sample 2	Test Statistic	Std. Error	Std. Test Statistic	Sig.	Adj. Sig.
CG 0°-DG 5°	-6.900	4.651	-1.483	0.138	1.000
CG 0°-DG 0°	-8.200	4.651	-1.763	0.078	0.779
CG 0°-DG 15°	-12.000	4.651	-2.580	0.010	0.099
CG 0°-DG 10°	-16.400	4.651	-3.526	<0.001	0.004
DG 5°-DG 0°	1.300	4.651	0.279	0.780	1.000
DG 5°-DG 15°	-5.100	4.651	-1.096	0.273	1.000
DG 5°-DG 10°	-9.500	4.651	-2.042	0.041	0.411
DG 0°-DG 15°	-3.800	4.651	-0.817	0.414	1.000
DG 0°-DG 10°	-8.200	4.651	-1.763	0.078	0.779
DG 15°-DG 10°	4.400	4.651	0.946	0.344	1.000

6 Discussion

This study investigates the biomechanical stability of hybrid hyrax appliances anchored with angle-stable DIRECT mini-implants. New insights into the biomechanical stability of DIRECT mini-implants, when used in conjunction with the hybrid hyrax appliance for palatal expansion, revealed greater stability and lower deformation under load than conventionally anchored hybrid hyrax appliances with traditional screw-mounted mini-implants. The findings obtained in this context are of great interest both for the theoretical understanding of orthodontic biomechanics and for practical clinical application, as they can contribute to increasing the effectiveness of future therapies.

Since the inception of orthodontics, anchorage has been a critical and fundamental aspect of desired tooth movement. A comprehensive understanding of biomechanics is essential for providing suitable treatment to patients. The application of compression and tensile forces to facilitate tooth movement consequently requires the use of an anchorage unit. (Umalkar et al., 2022). Metal implants and their biomechanics for anchorage have been researched since 1945 (Ritto, 2004), but have only been used in practice from 1983 onwards (Block et al., 1998, Creekmore and Eklund, 1983). The introduction of temporary anchorage devices, e.g., mini-implants, effected important changes in the orthodontic field by addressing the limitations of conventional anchorage because they are multi-effective (Ren, 2009), minimally invasive, and cost-effective (Araujo-Monsalvo et al., 2019, Costa et al., 1998, Kanomi, 1997) and therefore improve treatment opportunities.

6.1 Discussion of Results

The results of this study indicate that angle-stable mini-implants provide superior biomechanical behavior in vitro regarding maximum force threshold, deformation limit, and activation compared to right-angle-inserted Benefit Standard mini-implants concerning the expansion screw coupling type. Hence, the null hypotheses formulated in this dissertation are rejected and the alternative hypotheses are accepted (Fig. 20 and 21). Benefit DIRECT mini-implants offer the distinct advantage of being inserted after the appliance (“appliance first workflow”), eliminating issues with misfitting components. Although the unguided insertion of DIRECT mini-implants in clinical practice can result

in minor misangulations, our *in vitro* analysis demonstrated no compromise in mini-implant performance. In fact, misangulated DIRECT-mini-implants showed higher resistance to expansion forces, greater deformation limits, and longer activation distances compared to the Standard Benefit mini-implants inserted perpendicularly (Tables 12 and 16). These findings led to the rejection of the null hypotheses and highlighted the biomechanical superiority of the DIRECT system. Notably, the insertion angles of the DIRECT mini-implants had no adverse impact on mechanical performance. The stability of DIRECT mini-implants is ascribed to the angle-stable polyaxially thread design, which enhances the implant-abutment interface and heightens load transfer to the bone. The data from this study reinforce previous findings in the field of MARPE, which suggest that hybrid hyrax appliances supported by angle-stable mini-implants offer substantial improvements over conventional appliances in achieving controlled skeletal expansion (Wilmes et al., 2010).

Maxillary transverse deficiency, a frequently encountered finding in orthodontics, with a prevalence of up to 10%, often requires skeletal expansion by rapid maxillary expansion (RME) (Haas, 1970, Akyalcin and Alev, 2023), especially in younger patients. Although traditional RME is effective, it is associated with undesired dental side effects such as buccal tipping of the molars, bone loss, and dehiscences. These issues have been discussed intensively in orthodontic meta-studies (Greenbaum and Zachrisson, 1982, Copello et al., 2020, Kapetanović et al., 2021, Garrett et al., 2008, Odenrick et al., 1982). In contrast, Wilmes et al. (2010) introduced the concept of mini-implant assisted expansion (Wilmes et al., 2010). In 2010, Lee et al. (2010) treated a 20-year-old patient with severe transverse discrepancy and mandibular prognathism (Lee et al., 2010). Before undergoing orthognathic surgery, the patient had been treated with a mini-implant-assisted expansion device, resulting in an effective treatment outcome. The BMX expander, a skeletal anchorage system supported by only two mini-implants, was proposed by Wilmes et al. in 2021 and further simplifies the MARPE approach (Wilmes et al., 2021). Multiple studies have highlighted the advantages and confirmed its biomechanical and clinical efficacy of MARPE over traditional RME techniques, documenting a higher skeletal effect of the hybrid hyrax as well as a more controlled and effective parallel expansion (Choi et al., 2016, Lim et al., 2017, Oliveira et al., 2021a, Chun et al., 2022, Park et al., 2017, Jia et al., 2021, Ngan et al., 2018, Yilmaz et al., 2015,

Lin et al., 2015, Lagravère et al., 2010, Akin et al., 2016, Celenk-Koca et al., 2018). For instance, in a finite element study, MacGinnis et al. (2014) analyzed how RPE with conventional tooth-borne hyrax appliance and MARPE affect the transverse expansion stress and displacement in the craniofacial complex. By simulating forces on the maxilla, the researchers showed that MARPE caused less rotation of the maxilla with unwanted side effects compared to conventional methods (MacGinnis et al., 2014).

In another clinical comparative study between the hybrid and the conventional hyrax expanders, only a “tendency” towards improved alveolar bone morphology after expansion was observed (Silva et al., 2024).

Due to “increased comfort” for the patients and clinicians, Wilmes et al. (2022) suggest that the “TADs first” insertion method of MARPE hybrid-hyrax systems tends to improve patients’ compliance (Wilmes, 2022) (p. 3f).

Earlier, Cantarella et al. (2017) reported significant improvements in achieving desired skeletal expansion outcomes by the precise positioning and stability of mini-implants (Cantarella et al., 2017). The results of this study point out that the DIRECT group demonstrated not only superior expansion but also less variability in results, underscoring the reliability of the angle-stable mini-implants. Additionally, based on CBCT scans, Echarri-Nicolás et al. (2024) showed the more parallel opening of the mid-palatal suture with mini-implant assisted rapid palatal expanders, which underscores the benefit of MARPE appliances (Echarri-Nicolás et al., 2024).

MARPE has generated significant research due to its promising effects on nose breathing (Anéris et al., 2023, Bazargani et al., 2018, Benetti et al., 2024, Dominguez-Mompell et al., 2024, Echarri-Nicolás et al., 2023, Hur et al., 2017, Mehta et al., 2021, Li et al., 2023, Prévé and García Alcázar, 2022, Yi et al., 2020, Zeng et al., 2023). Dominguez-Mompell et al. (2024) postulated that maxillary skeletal expansion offers a non-surgical alternative for achieving orthopedic expansion in adults patients, thereby supporting its benefits in addressing upper airway obstruction (Dominguez-Mompell et al., 2024). Additionally, Brunetto et al. (2022) indicated that MARPE has a positive impact on obstructive sleep apnea by expanding the midface as well as the oral and nasal cavities, reducing airflow resistance, and consequently improving quality of life (Brunetto et al., 2022).

Earlier research from Déjardin et al. (2006) reported that the biomechanical properties of hourglass-shaped interlocking implants with a self-tapping tapered locking design

eliminate the instability associated with current “interlocking nails” and allow resistance to major stresses, such as torsion, compression, and bending in surgery (Déjardin et al., 2006).

The biomechanical stability of the connection between the appliance and the mini-implant is crucial for the success of orthodontic treatment. Conventional mini-implant composite methods have disadvantages in terms of the need for precise insertion techniques and the associated susceptibility to errors. The results of this scientific study expand on these findings by highlighting the advantages of angle-independent mini-implants achieved by higher maximum forces, a more even distribution of load, and a significant reduction in deformation.

6.2 Discussion on Angle- and Connection-Dependent Displacement

A critical aspect of the biomechanical integration of mini-implants is the type of connection of the mini-implant and the abutment of the expansion screw, as well as its influence on force transmission and bone response at the midpalatal suture. Some studies analyzed the connection between different mini-implants and orthodontic appliances and compared their stability (de la Iglesia et al., 2018, Walter et al., 2023). Oliveira et al. (2021) used the finite element method to evaluate the stresses and displacements of different numbers of mini-implants in an expansion appliance during a maxillary expansion. They showed that larger forces acted on the mini-implant than on the expansion arm of the appliance (Oliveira et al., 2021b).

The determination of whether mini-implants are inserted either straight or at an angle, as well as the associated complications during the expansion process, are determined by biomechanics. Straight mini-implants, such as CG0° and DG0°, are distinguished by their predominant axial force transmission, which primarily compresses the bone and applies only minimal tangential forces to the peri-implant bone (Sakamaki et al., 2022). This reduces the risk of microfractures and stress zones (Sana et al., 2020), while concurrently reducing bone displacement in comparison to angled mini-implants like DG5°, DG10°, or DG15° (Fig. 20 and 21).

These outcomes align with previous studies investigating the improvement in anchorage effectiveness through innovative implant designs. Numerous orthodontic researchers

have investigated the biomechanical properties of traditional mini-implants in various designs (Consolaro and Romano, 2014, de Aguiar et al., 2015, de la Iglesia et al., 2018, Déjardin et al., 2006, Edwards and Mah, 2010, Elkolaly and Hasan, 2022, Florvaag et al., 2010). For instance, Kim et al. (2009) compared the mechanical properties of traditional mini-implants of different shapes, such as cylindrical, conical, and double-threaded implants, in lengths of 6 mm and 8 mm, with respect to insertion and removal torque. The findings showed that the double-threaded design exhibited the highest removal torque and superior mechanical stability, whereas the cylindrical design recorded the lowest torques. However, the double-threaded shape could be optimized by reducing the insertion time to lessen stress on the surrounding tissue (Kim et al., 2009).

A factor in assessing the success of orthodontic appliances and the stability of implants is “the mechanical interlocking between the mini-implant and the bone” (Consolaro and Romano, 2014). Angulated mini-implants inherently generate tangential forces and additional shear stresses, which result in uneven bone displacement and increased strain on cortical bone structures (Udomsawat et al., 2019). Nonetheless, the mechanical limits are constrained by the rigidity of the hyrax expander, bone quality, and material deformation within the implant-abutment system.

In our setup, standard Benefit mini-implants (CG0°) reached the threshold of plastic deformation at 80-100 N, while DIRECT mini-implants remained within elastic limits for a longer, superior force tolerance (Fig. 13). Recent research by Navarrete et al. (2024) comparing cemented abutment connections with screwed abutment connections in a torsion-resistant in vitro test showed that screw-type abutment connection systems exhibit less flexural strength and torsional resistance against tangential loads. (Navarrete et al., 2024) This further emphasizes the significance of connection design. Our findings support this conclusion, highlighting the importance of precise dimensioning and material selection for the connection components of hybrid hyrax appliances to ensure biomechanical integrity during expansion.

Mini-implants with a direct mechanism constitute a novel approach in orthodontic therapy, first described by Wilmes et al. (2022) as an "appliance-first-implants-second" protocol: Inserting the appliance prior to mini-implantation ("appliance first") enables enhanced precision and effectiveness when contrasted with conservative methods (Wilmes, 2022) (p. 4). The examination of the DIRECT mini-implants featuring a

polyaxial thread in this study revealed that the mini-implants, when mounted by the abutment of the BMX expansion screw, establish a rigid and stable connection prior to any intended expansive treatment. In contrast to the Benefit Standard Mini-Implant System, where a fixation screw connects the expander, the DIRECT mechanism reduces the risk of unwanted movements between the mini-implant's head and the orthodontic appliance. This is demonstrated in our study results, which show a significantly higher tolerance threshold for maximum forces and deformation in mini-implant-assisted palatal expansion.

Palatal expansion in adults faces increased biomechanical challenges due to higher bone density and more complex midpalatal suture interdigitation (Naveda et al., 2022). Under these conditions, standard Benefit mini-implants, which have lower thresholds for plastic deformation, may present problems because of irreversible deformations that can compromise overall stability and function. The DIRECT mini-implant's angle-stable connection to the abutment via the polyaxial thread and greater load capacity, is better suited for this population. Its polyaxial interface helps maintain mechanical stability even under high forces and angulation (Fig. 20 and 21).

Due to a variety of anatomical conditions, the correct position for the insertion of mini-implants is often challenging (Consolaro and Romano, 2014, Hourfar et al., 2015a, Wilmes et al., 2006). Becker et al. (2019) investigated optimal angles and positions for the insertion of orthodontic mini-implants in the anterior palate based on a CBCT scan analysis of 30 patients. They showed that a posteriorly oriented inclination of the mini-implants in the anterior insertion area and an anterior inclination of the mini-implants in the posterior insertion area led to better stability-relevant bone heights, while the inclination angle in the mid-median plane had no significant influence (Becker et al., 2019). The study provided important insights into the optimal insertion position and insertion inclination. At an unfavorable implant angle, suboptimal force transfer to the bone occurs, which can lead to instability (Tatli et al., 2019). The results in this dissertation support the hypothesis that angle-independent mini-implants minimize these problems. The flexible adjustment of insertion at different insertion angles is particularly important in complex cases where optimal implant positioning is limited by anatomical variations of the palate (Kang et al., 2020).

Optimizing load capacity through the flexible adjustment of the targeted angular deviation without compromising device stability improves the efficiency and safety of the treatment. This finding is consistent with an *in vitro* comparative study analyzing the biomechanical loading of polyaxial locking plates (Hebert-Davies et al., 2013). Monoaxial screws recorded a 60% reduction in force absorption at an angular deviation of 10 degrees, whereas polyaxial screws showed a smaller reduction in load capacity at the same angle. These results suggest that the flexibility of polyaxial systems can provide surgical flexibility and, therefore, be advantageous; however, this can also be associated with stability deficits, particularly at extreme angles. Regarding the questions addressed in this dissertation, similar results are confirmed, indicating that a slight adjustment of the angle by 10 or 15 degrees leads to a significant improvement in the load resistance of the mini-implants. These results emphasize the positive aspects of a polyaxial thread design, especially in situations where anatomically determined variability in orthodontic insertion is necessary.

Studies often focus primarily on the biomechanical properties of the mini-implants and less on their interaction with the combined orthodontic appliance. Various methods already exist that investigate the connection between different mini-implants and orthodontic appliances and compare their stability (de la Iglesia et al., 2018, Walter et al., 2023). Oliveira et al. (2021) employed a finite element method to simulate the stresses and displacements of various mini-implants used in conjunction with an expansion device during palatal expansion, demonstrating that the forces acting on the mini-implant are greater than those acting on the expansion arm of the appliance (Oliveira et al., 2021b). Uneven load distribution on the mini-implants leads to instabilities in the orthodontic appliance and consequently to a reduction in treatment efficiency. In a finite element method, Benaissa et al. (2020) investigated how orthodontic forces influence the stress distribution on mini-implants, periodontal tissues, and the tooth-bracket interface. It was found that uneven stress distribution, particularly in the area of the mini-implant neck and the alveolar bone region, can lead to unstable conditions, bone loss, and, consequently, material failure (Benaissa et al., 2020). Our experiments revealed local stress peaks, particularly in the Benefit Standard group, in the area of the mini-implant necks, which consequently weakened and loosened the connection between the fixation screws and the abutments. The resulting loosening of the BMX expansion screw from the mini-implants

in the artificial bone is the reason for a lower load limit in the results of our study and suggests that wedging in the abutment without a fixation screw is the more favorable biomechanical connection in the Benefit DIRECT group. The improved stability of the angle-stable Benefit DIRECT mini-implants could minimize undesirable complications such as asymmetric palatal expansion or excessive loading of individual teeth. The biomechanical advantages of the angle-stable mini-implants are primarily manifested in a better distribution of the occurring forces and a reduction in stress peaks at the anchorage points. This is consistent with the *in vitro* analysis by de la Iglesia et al. (2018), which shows that insufficiently rigid anchorage to the hybrid hyrax expansion elements results in excessive stresses at the anchorage points and thus an increased risk of implant failure (de la Iglesia et al., 2018). The results of this study confirm these observations by demonstrating that the mechanical integrity of the device is increased.

6.3 Discussion on Limitations of the Experimental Setup

Although the present results are promising, some limitations of the study must be considered. A controlled, *in vitro* laboratory environment was chosen to evaluate the biomechanical properties of DIRECT mini-implants during expansion. This approach simulates forces and loads that cannot be studied in humans. *In vitro* studies are a fundamental principle in biomedical research, providing valuable insights into the mechanical properties and performance of medical devices, including orthodontic mini-implants and expanders. They allow for controlled comparison and reproducibility but cannot fully replicate the complexity of the clinical environment. Artificial bone, while standardized, lacks the anatomical variability of human tissue. Load patterns were simplified, not accounting for multidirectional forces from masticatory function or individual differences.

The mini-implants used in our experimental *in vitro* study on the biomechanical stability of the angle-modified mini-implants combined with the hybrid hyrax appliance were selected based on the literature and on clinical practice recommendations for maxillary expansion measuring 2.0 mm in diameter and 9.0 mm in length (Patiño et al., 2024). Kovuru et al. (2023) concluded in their three-dimensional finite element study that stress decreases with longer implants, (Kovuru et al., 2023) and Sadr Haghighi et al. (2019)

postulated that an increase in the diameter of the mini-implants results in better primary stability (Sadr Haghghi et al., 2019). Therefore, the length and diameter of the mini-implants were adapted accordingly in our study.

The primary stability of the mini-implants after insertion in the bone is the prerequisite for reliable maximum force measurement in our study. Studies show that the primary stability of mini-implants is influenced by factors such as bone morphology and quality, implant design, implant length, implant diameter, surgical procedure, insertion torque, and pre-drilling (Bilhan et al., 2010, Chatzigianni et al., 2011, Chhatwani et al., 2022, Copello et al., 2021b, Hong et al., 2012, Katalinic et al., 2017, Möhlhenrich et al., 2015a, Möhlhenrich et al., 2020a, Wilmes et al., 2008a). A limitation of the experimental study is the use of artificial bone. To conduct controlled comparisons between the groups in our study, we used solid artificial bone, which resembles the average cortical bone of the human palatine bone. The advantages and disadvantages of the established artificial bone from Sawbone (Sawbone, Pacific, USA) regarding its use in comparative studies to assess implant stability have been discussed in numerous scientific studies (Calvert et al., 2010, Hosein et al., 2016). Scientific studies describe the mechanical properties of polyurethane artificial bone as mimicking human maxillary bone (Devlin et al., 1998), which is more homogeneously dense than bovine cadaver bone (Calvert et al., 2010). The properties of natural bone tissue vary about mineralization in different patient ages. The results cannot be extrapolated to in vivo conditions, which is why the effects of the implants' behavior in real-life application situations can vary.

Due to the hardness of the artificial bone, a pilot hole was drilled prior to mini-implantation. The beneficial effects of pre-drilling on the osseointegration of mini-implants are described in the literature (Shin et al., 2012). Wilmes et al. (2009) investigated the influence of insertion depth and pre-drill diameter on the primary stability of mini-implants, measured by insertion torque. It was shown that greater insertion depths lead to a higher torque, but larger diameters of the pre-drilling correlate with a lower torque (Wilmes and Drescher, 2009). An optimal diameter for the pre-drilling is necessary to avoid mini-implant fractures and ensure sufficient orthodontic anchorage (Wilmes and Drescher, 2011). Higher success rates in orthodontic anchorage and the necessity of pre-drilling when inserting self-tapping mini-implants versus self-

drilling mini-implants are controversially discussed in the literature (Chen et al., 2008). Self-tapping mini-implants, in comparison to self-drilling mini-implants, have a special cutting edge and thus a thread profile that enables direct insertion into the bone. Yadav et al. (2012) evaluated the influence of insertion techniques for self-tapping (without pilot drilling) versus self-drilling (with pilot drilling) mini-implants on microfracture formation and propagation in the cortical bone structure of the maxilla and mandible in adult dogs. The results showed that a technique without pre-drilling for self-tapping mini-implants caused more microfractures and greater crack densities in the bone (Yadav et al., 2012). Pilot drilling is also necessary for self-drilling mini-implants because they have a higher insertion torque (Su et al., 2009).

In human palatal bone, pre-drilling is generally not necessary in children because the bone is not yet fully mineralized (Braga et al., 2023). In adults, however, the risk of peri-implant microfracture increases with age due to higher bone density. Factors such as the high density and quality of the artificial bone used in this study negatively impacted our pilot tests without pre-drilling and led to increased resistance during mini-implantation. Although pre-drilling was performed, the risk of uncontrolled fractures of the artificial bone and excessive deformation during insertion was increased. A recent study revealed that excessive insertion torque, exceeding 35 N, increases the risk of microdamage in the peri-implant bone (Ceddia et al., 2025).

The implantation of implants without pre-drilling may cause an increase in bone temperature (Gupta et al., 2012), especially without water cooling. Pre-drilling reduces mechanical stress and thus reduces overheating in the bone. In a review analyzing methods to minimize heat damage during implantation, Möhlhenrich et al. (2015) concluded that standardized conditions, including a contact pressure of 2 kg, a rotational speed of 1500 rpm, water cooling, and infrared thermography, are beneficial (Möhlhenrich et al., 2015b).

Based on these scientific findings, pre-drilling was performed in our study to create reproducible conditions. To further enable comparisons between the Benefit standard mini-implants and DIRECT mini-implants, the same diameter (1.4 mm) for the pre-drilling and the same pre-drilling depth of 6 mm were used for all mini-implants in our

study, thus ensuring optimal stability of all mini-implants in the artificial bone prior to loading tests.

Pre-drilling in our study was performed using specially manufactured drill guides manufactured using the CAD/CAM process. After this, the mini-implantation could be performed at pre-defined angles (0°, 5°, 10°, 15°) up to a depth of 9 mm using specially manufactured insertion double guides, which were also manufactured using the CAD/CAM process. The use of CAD/CAM-manufactured insertion templates for mini-implant positioning in this study maximizes repeatability in the trials. This optimizes the targeted positioning of the mini-implants through the expansion screw abutments and thus the biomechanical efficiency of the appliance. Precise preoperative diagnostics and planning, utilizing virtual planning software for guided implant surgery, are now standard in modern dental prosthodontics. This approach integrates computed tomography data and virtual models for implant planning and the fabrication of surgical guides. The accuracy of transferring implant positions depends on the quality of data processing, artifact suppression, and registration accuracy (Flügge et al., 2022, Kernen et al., 2020). Orthodontic treatment has also been revolutionized by novel methods for virtual planning prior to mini-implant placement (Cantarella et al., 2020). Purely mini-implant-supported RPEs require CAD/CAM-manufactured insertion guides (Wilmes et al., 2022b).

Furthermore, minor errors may have occurred when tightening and re-tightening the bone blocks with the mini-implants and the expander in the vise. A slight deformation of the test setup may have occurred during measurement, as the test was performed under maximum load. Sensor measurement errors occurred twice, requiring these measurements to be repeated. Errors with the socket electrodes might also have been possible. Additionally, the expansion screws could have affected the results. All of these factors together may limit the generalizability of the findings.

Additionally, other aspects such as inadequate abutment welding can influence the mechanical loading properties (Rodrigues et al., 2017), as the elastic load-bearing capacity of the entire hybrid hyrax system directly influences the effectiveness of the expansion. The tests revealed clear plastic deformation of the laser weld seam, which only occurred at higher forces with the DIRECT system. It is being considered whether the results would have been different if the laser weld between the abutment and the BMX

expansion screw had been stronger. The possible reason for the lower load resistance in the control group is a loosened connection between the Benefit Standard mini-implant and the abutment of the BMX expansion screw.

Hybrid hyrax appliances are characterized by complex bone displacement, as they utilize force transmission through both skeletal anchorage via mini-implants and dental anchorage via the teeth, in contrast to systems that rely exclusively on one type of anchorage. Additionally, skeletal anchorage in hybrid systems interacts with dentoalveolar anchorage, generating complex bending moments. This study focused solely on skeletal contributions and excluded these additional influences, which should be considered in further in vivo investigations.

6.4 Clinical Conclusion

The findings of the experimental study in this dissertation underscore the potential of angle-stable DIRECT Mini-Implants to improve the clinical efficiency and safety of palatal expansion. In the future, mini-implants are expected to continue playing a significant role in enhancing orthodontic treatment outcomes and predictability. MARPE has emerged as a highly effective alternative to conventional RPE or sometimes SARPE. The stability of the mini-implant and its connection to the appliance is mandatory for treatment success, especially during the initial, high-force phase of expansion. In comparison to the well-established, standard Benefit mini-implant, this study confirms that Benefit DIRECT mini-implants provide superior biomechanical properties, even if inserted at angulations of up to ± 15 degrees (Fig. 20 and 21). Due to the possibility of flexible angle adjustment and the resulting improved load distribution, DIRECT mini-implants can be particularly beneficial in clinically challenging cases with difficult anatomical conditions.

Future in vivo studies should validate the results and the biomechanical efficiency and safety of the DIRECT mini-implants in clinical applications further to optimize orthodontic palatal expansion systems and their anchorage techniques. An investigation of the long-term stability of DIRECT mini-implants during palatal expansion and their impact on clinical treatment success would be interesting. Further in vitro analyses of micromovement, anchorage force under different loading, or a combination of Benefit

Standard mini-implants with DIRECT mini-implants in a purely mini-implant-assisted palatal expansion should be conducted.

Both mini-implants were evaluated alongside a skeletally anchored expander (BMX). The appliance-first approach simplifies clinical procedures and reduces errors related to appliance fit. In conclusion, the DIRECT system is a promising option for modern skeletal expansion protocols in clinical practice.

7 References

1. AKIN, M., AKGUL, Y. E., ILERI, Z. & BASCIFTCI, F. A. 2016. Three-dimensional evaluation of hybrid expander appliances: A pilot study. *Angle Orthod*, 86, 81-6.
2. AKYALCIN, S. & ALEV, Y. 2023. Clinical advances in maxillary skeletal expansion and introduction of a new MARPE concept. *J Esthet Restor Dent*, 35, 291-298.
3. ANÉRIS, F. F., EL HAJE, O., ROSÁRIO, H. D., DE MENEZES, C. C., FRANZINI, C. M. & CUSTODIO, W. 2023. The effects of miniscrew-assisted rapid palatal expansion on the upper airway of adults with midpalatal suture in the last two degrees of ossification. *J World Fed Orthod*, 12, 150-155.
4. ANGELL, D. 1860. Treatment of irregularity of the permanent or adult teeth. *Dent Cosmos*. Dent Cosmos.
5. ARAÚJO, M. C., BOCATO, J. R., OLTRAMARI, P. V., DE ALMEIDA, M. R., CONTI, A. C. & FERNANDES, T. M. 2020. Tomographic evaluation of dentoskeletal effects of rapid maxillary expansion using Haas and Hyrax palatal expanders in children: A randomized clinical trial. *J Clin Exp Dent*, 12, e922-e930.
6. ARAUJO-MONSALVO, V. M., GONZÁLEZ-ARÉAS, M. G., MARTÍNEZ-CORIA, E., FLORES-CUAMATZI, E., ARAUJO-MONSALVO, B. & DOMÍNGUEZ-HERNÁNDEZ, V. M. 2019. Effect of insertion angle on the stability of orthodontic mini-implants in a rabbit tibia model: A finite element analysis. *Cir Cir*, 87, 190-195.
7. ASSAD-LOSS, T. F., KITAHARA-CÉIA, F. M. F., SILVEIRA, G. S., ELIAS, C. N. & MUCHA, J. N. 2017. Fracture strength of orthodontic mini-implants. *Dental Press J Orthod*, 22, 47-54.
8. BAZARGANI, F., MAGNUSON, A. & LUDWIG, B. 2018. Effects on nasal airflow and resistance using two different RME appliances: a randomized controlled trial. *Eur J Orthod*, 40, 281-284.
9. BECKER, K., UNLAND, J., WILMES, B., TARRAF, N. E. & DRESCHER, D. 2019. Is there an ideal insertion angle and position for orthodontic mini-implants in the anterior palate? A CBCT study in humans. *Am J Orthod Dentofacial Orthop*, 156, 345-354.
10. BENAÏSSA, A., MERDJI, A., BENDJABALLAH, M. Z., NGAN, P. & MUKDADI, O. M. 2020. Stress influence on orthodontic system components under simulated treatment loadings. *Comput Methods Programs Biomed*, 195, 105569.
11. BENETTI, M., MONTRESOR, L., CANTARELLA, D., ZERMAN, N. & SPINAS, E. 2024. Does Miniscrew-Assisted Rapid Palatal Expansion Influence Upper Airway in Adult Patients? A Scoping Review. *Dent J (Basel)*, 12.
12. BETTS, N. J., VANARSDALL, R. L., BARBER, H. D., HIGGINS-BARBER, K. & FONSECA, R. J. 1995. Diagnosis and treatment of transverse maxillary deficiency. *Int J Adult Orthodon Orthognath Surg*, 10, 75-96.
13. BILHAN, H., GECKILI, O., MUMCU, E., BOZDAG, E., SÜNBUĞLU, E. & KUTAY, O. 2010. Influence of surgical technique, implant shape and diameter on the primary stability in cancellous bone. *J Oral Rehabil*, 37, 900-7.

14. BLOCK, M. S., ALMERICO, B., CRAWFORD, C., GARDINER, D. & CHANG, A. 1998. Bone response to functioning implants in dog mandibular alveolar ridges augmented with distraction osteogenesis. *Int J Oral Maxillofac Implants*, 13, 342-51.
15. BRAGA, C., POZZAN, L., CIOTOLA, C., VIGANONI, C., TORELLI, L. & CONTARDO, L. 2023. Bone quality in relation to skeletal maturation in palatal miniscrews insertion sites. *Am J Orthod Dentofacial Orthop*, 164, 406-415.
16. BRUNETTO, D. P., MOSCHIK, C. E., DOMINGUEZ-MOMPELL, R., JARIA, E., SANT'ANNA, E. F. & MOON, W. 2022. Mini-implant assisted rapid palatal expansion (MARPE) effects on adult obstructive sleep apnea (OSA) and quality of life: a multi-center prospective controlled trial. *Prog Orthod*, 23, 3.
17. BRUNETTO, D. P., SANT'ANNA, E. F., MACHADO, A. W. & MOON, W. 2017. Non-surgical treatment of transverse deficiency in adults using Microimplant-assisted Rapid Palatal Expansion (MARPE). *Dental Press J Orthod*, 22, 110-125.
18. BüyüKçAVUŞ, M. H. 2019. Alternate Rapid Maxillary Expansion and Constriction (Alt-RAMEC) protocol: A Comprehensive Literature Review. *Turk J Orthod*, 32, 47-51.
19. CALVERT, K. L., TRUMBLE, K. P., WEBSTER, T. J. & KIRKPATRICK, L. A. 2010. Characterization of commercial rigid polyurethane foams used as bone analogs for implant testing. *J Mater Sci Mater Med*, 21, 1453-61.
20. CANTARELLA, D., DOMINGUEZ-MOMPELL, R., MALLYA, S. M., MOSCHIK, C., PAN, H. C., MILLER, J. & MOON, W. 2017. Changes in the midpalatal and pterygopalatine sutures induced by micro-implant-supported skeletal expander, analyzed with a novel 3D method based on CBCT imaging. *Prog Orthod*, 18, 34.
21. CANTARELLA, D., SAVIO, G., GRIGOLATO, L., ZANATA, P., BERVEGLIERI, C., LO GIUDICE, A., ISOLA, G., DEL FABBRO, M. & MOON, W. 2020. A New Methodology for the Digital Planning of Micro-Implant-Supported Maxillary Skeletal Expansion. *Med Devices (Auckl)*, 13, 93-106.
22. CARLSON, C., SUNG, J., MCCOMB, R. W., MACHADO, A. W. & MOON, W. 2016. Microimplant-assisted rapid palatal expansion appliance to orthopedically correct transverse maxillary deficiency in an adult. *Am J Orthod Dentofacial Orthop*, 149, 716-28.
23. CEDDIA, M., MONTESANI, L., COMUZZI, L., CIPOLLINA, A., DEPORTER, D. A., DI PIETRO, N. & TRENTADUE, B. 2025. The Influence of Insertion Torque on Stress Distribution in Peri-Implant Bones Around Ultra-Short Implants: An FEA Study. *J Funct Biomater*, 16.
24. CELENK-KOCA, T., ERDINC, A. E., HAZAR, S., HARRIS, L., ENGLISH, J. D. & AKYALCIN, S. 2018. Evaluation of miniscrew-supported rapid maxillary expansion in adolescents: A prospective randomized clinical trial. *Angle Orthod*, 88, 702-709.
25. CHAMBERLAND, S. 2023. Maxillary expansion in nongrowing patients. Conventional, surgical, or miniscrew-assisted, an update. *J World Fed Orthod*, 12, 173-183.

26. CHATZIGIANNI, A., KEILIG, L., REIMANN, S., ELIADES, T. & BOURAUDEL, C. 2011. Effect of mini-implant length and diameter on primary stability under loading with two force levels. *Eur J Orthod*, 33, 381-7.
27. CHEN, Y., SHIN, H. I. & KYUNG, H. M. 2008. Biomechanical and histological comparison of self-drilling and self-tapping orthodontic microimplants in dogs. *Am J Orthod Dentofacial Orthop*, 133, 44-50.
28. CHHATWANI, S., KOUJI-DIEHL, O., KNIHA, K., MODABBER, A., HÖLZLE, F., SZALMA, J., DANESH, G. & MÖHLHENRICH, S. C. 2022. Significance of bone morphology and quality on the primary stability of orthodontic mini-implants: in vitro comparison between human bone substitute and artificial bone. *J Orofac Orthop*.
29. CHOI, S. H., SHI, K. K., CHA, J. Y., PARK, Y. C. & LEE, K. J. 2016. Nonsurgical miniscrew-assisted rapid maxillary expansion results in acceptable stability in young adults. *Angle Orthod*, 86, 713-20.
30. CHUN, J. H., DE CASTRO, A. C. R., OH, S., KIM, K. H., CHOI, S. H., NOJIMA, L. I., NOJIMA, M. & LEE, K. J. 2022. Skeletal and alveolar changes in conventional rapid palatal expansion (RPE) and miniscrew-assisted RPE (MARPE): a prospective randomized clinical trial using low-dose CBCT. *BMC Oral Health*, 22, 114.
31. CLARENBACH, T. H., WILMES, B., IHSEN, B., VASUDAVAN, S. & DRESCHER, D. 2017. Hybrid hyrax distalizer and mentoplate for rapid palatal expansion, class III treatment, and upper molar distalization. *J Clin Orthod*, 51, 317-325.
32. CONSOLARO, A. & ROMANO, F. L. 2014. Reasons for mini-implants failure: choosing installation site should be valued! *Dental Press J Orthod*, 19, 18-24.
33. COPELLO, F. M., BRUNETTO, D. P., ELIAS, C. N., PITHON, M. M., COQUEIRO, R. S., CASTRO, A. C. R. & SANT'ANNA, E. F. 2021a. Miniscrew-assisted rapid palatal expansion (MARPE): how to achieve greater stability. In vitro study. *Dental Press J Orthod*, 26, e211967.
34. COPELLO, F. M., MARAÑÓN-VÁSQUEZ, G. A., BRUNETTO, D. P., CALDAS, L. D., MASTERSON, D., MAIA, L. C. & SANT'ANNA, E. F. 2020. Is the buccal alveolar bone less affected by mini-implant assisted rapid palatal expansion than by conventional rapid palatal expansion?-A systematic review and meta-analysis. *Orthod Craniofac Res*, 23, 237-249.
35. COPELLO, F. M., SILVEIRA, A. M., CASTRO, A. C. R., LOPES, R. T., KO, F., SUMNER, D. R. & SANT'ANNA, E. F. 2021b. In-vitro trabecular bone damage following mono- and bicortical mini implants anchorage in mini-implant assisted rapid palatal expansion (MARPE). *Int Orthod*, 19, 243-251.
36. COSTA, A., RAFFAINL, M. & MELSEN, B. 1998. Miniscrews as orthodontic anchorage: a preliminary report. *Int J Adult Orthodon Orthognath Surg*, 13, 201-9.
37. CREEKMORE, T. D. & EKLUND, M. K. 1983. The possibility of skeletal anchorage. *J Clin Orthod*, 17, 266-9.
38. DAL PAZ, J., DALLEPIANE, F. G., DA SILVA, A., BELTRAMI, L. V. R., HAUPT, W. & TRENTIN, M. S. 2025. Effects of corrosion on orthodontic mini-implants related to removal torque fracture resistance. *J Clin Exp Dent*, 17, e273-e279.

39. DE AGUIAR, A. M., BRAMANTE, F. S., DE AGUIAR, A. M. & PINZAN-VERCELINO, C. R. 2015. Evaluation of Fracture Resistance of Orthodontic Mini-implants in the Transmucosal Profile Region. *J Contemp Dent Pract*, 16, 372-5.
40. DE LA IGLESIA, G., WALTER, A., DE LA IGLESIA, F., WINSAUER, H. & PUIGDOLLERS, A. 2018. Stability of the anterior arm of three different Hyrax hybrid expanders: an in vitro study. *Dental Press J Orthod*, 23, 37-45.
41. DE OLIVEIRA, C. B., AYUB, P., LEDRA, I. M., MURATA, W. H., SUZUKI, S. S., RAVELLI, D. B. & SANTOS-PINTO, A. 2021. Microimplant assisted rapid palatal expansion vs surgically assisted rapid palatal expansion for maxillary transverse discrepancy treatment. *Am J Orthod Dentofacial Orthop*, 159, 733-742.
42. DéJARDIN, L. M., LANSDOWNE, J. L., SINNOTT, M. T., SIDEBOTHAM, C. G. & HAUT, R. C. 2006. In vitro mechanical evaluation of torsional loading in simulated canine tibiae for a novel hourglass-shaped interlocking nail with a self-tapping tapered locking design. *Am J Vet Res*, 67, 678-85.
43. DEVLIN, H., HORNER, K. & LEDGERTON, D. 1998. A comparison of maxillary and mandibular bone mineral densities. *J Prosthet Dent*, 79, 323-7.
44. DOMINGUEZ-MOMPELL, R., ZHANG, B., PAREDES, N., COMBS, A., ELKENAWY, I., SFOGLIANO, L., FIJANY, L., COLAK, O., ROMEROMAROTO, M. & MOON, W. 2024. Breathing changes following mini-implant-supported maxillary skeletal expander treatment in late adolescent or adult patients : Assessment of objective and subjective functional breathing changes. *J Orofac Orthop*.
45. DOMINGUEZ-MOMPELL, R., ZHANG, B., PAREDES, N., COMBS, A., ELKENAWY, I., SFOGLIANO, L., FIJANY, L., COLAK, O., ROMEROMAROTO, M. & MOON, W. 2025. Breathing changes following mini-implant-supported maxillary skeletal expander treatment in late adolescent or adult patients : Assessment of objective and subjective functional breathing changes. *J Orofac Orthop*, 86, 248-258.
46. ECHARRI-NICOLÁS, J., GONZÁLEZ-OLMO, M. J., ECHARRI-LABIONDO, P. & ROMERO, M. 2023. Short-term outcomes in the upper airway with tooth-bone-borne vs bone-borne rapid maxillary expanders. *BMC Oral Health*, 23, 714.
47. ECHARRI-NICOLÁS, J., GONZÁLEZ-OLMO, M. J., ECHARRI-LOBIONDO, P., LAGRAVÈRE, M. & ROMERO, M. 2024. Tooth-Bone-Borne vs Bone-Borne Rapid Maxillary Expanders on Dentoskeletal Changes. *J Multidiscip Healthc*, 17, 1877-1886.
48. EDWARDS, C. W. & MAH, J. K. 2010. Mini-implant behavior to shear tensile forces in the porcine mandible. *World J Orthod*, 11, 362-8.
49. ELKOLALY, M. A. & HASAN, H. S. 2022. MH cortical screws, a revolutionary orthodontic TADs design. *J Orthod Sci*, 11, 53.
50. FAUL, F., ERDFELDER, E., LANG, A. G. & BUCHNER, A. 2007. G*Power 3: a flexible statistical power analysis program for the social, behavioral, and biomedical sciences. *Behav Res Methods*, 39, 175-91.

51. FELDMANN, I. & BAZARGANI, F. 2017. Pain and discomfort during the first week of rapid maxillary expansion (RME) using two different RME appliances: A randomized controlled trial. *Angle Orthod*, 87, 391-396.
52. FLORVAAG, B., KNEUERTZ, P., LAZAR, F., KOEBKE, J., ZÖLLER, J. E., BRAUMANN, B. & MISCHKOWSKI, R. A. 2010. Biomechanical properties of orthodontic miniscrews. An in-vitro study. *J Orofac Orthop*, 71, 53-67.
53. FLÜGGE, T., KRAMER, J., NELSON, K., NAHLES, S. & KERNEN, F. 2022. Digital implantology-a review of virtual planning software for guided implant surgery. Part II: Prosthetic set-up and virtual implant planning. *BMC Oral Health*, 22, 23.
54. GARRETT, B. J., CARUSO, J. M., RUNGCHARASSAENG, K., FARRAGE, J. R., KIM, J. S. & TAYLOR, G. D. 2008. Skeletal effects to the maxilla after rapid maxillary expansion assessed with cone-beam computed tomography. *Am J Orthod Dentofacial Orthop*, 134, 8-9.
55. GORRIERI, O., FINI, M., KYRIAKIDOU, K., ZIZZI, A., MATTIOLI-BELMONTE, M., CASTALDO, P., DE CRISTOFARO, A., NATALI, D., PUGNALONI, A. & BIAGINI, G. 2006. In vitro evaluation of bio-functional performances of Ghimas titanium implants. *Int J Artif Organs*, 29, 1012-20.
56. GREENBAUM, K. R. & ZACHRISSON, B. U. 1982. The effect of palatal expansion therapy on the periodontal supporting tissues. *Am J Orthod*, 81, 12-21.
57. GUPTA, N., KOTRASHETTI, S. M. & NAIK, V. 2012. A comparative clinical study between self tapping and drill free screws as a source of rigid orthodontic anchorage. *J Maxillofac Oral Surg*, 11, 29-33.
58. HAAS, A. J. 1970. Palatal expansion: just the beginning of dentofacial orthopedics. *Am J Orthod*, 57, 219-55.
59. HEBERT-DAVIES, J., LAFLAMME, G. Y., ROULEAU, D., CANET, F., SANDMAN, E., LI, A. & PETIT, Y. 2013. A biomechanical study comparing polyaxial locking screw mechanisms. *Injury*, 44, 1358-62.
60. HINO, C. T., PEREIRA, M. D., SOBRAL, C. S., KRENISKI, T. M. & FERREIRA, L. M. 2008. Transverse effects of surgically assisted rapid maxillary expansion: a comparative study using Haas and Hyrax. *J Craniofac Surg*, 19, 718-25.
61. HONG, J., LIM, Y. J. & PARK, S. O. 2012. Quantitative biomechanical analysis of the influence of the cortical bone and implant length on primary stability. *Clin Oral Implants Res*, 23, 1193-7.
62. HOSEIN, Y. K., SMITH, A., DUNNING, C. E. & TASSI, A. 2016. Insertion Torques of Self-Drilling Mini-Implants in Simulated Mandibular Bone: Assessment of Potential for Implant Fracture. *Int J Oral Maxillofac Implants*, 31, e57-64.
63. HOURFAR, J., KANAVAKIS, G., BISTER, D., SCHÄTZLE, M., AWAD, L., NIENKEMPER, M., GOLDBECKER, C. & LUDWIG, B. 2015a. Three dimensional anatomical exploration of the anterior hard palate at the level of the third ruga for the placement of mini-implants--a cone-beam CT study. *Eur J Orthod*, 37, 589-95.

64. HOURFAR, J., LUDWIG, B., BISTER, D., BRAUN, A. & KANAVAKIS, G. 2015b. The most distal palatal ruga for placement of orthodontic mini-implants. *Eur J Orthod*, 37, 373-8.
65. HUR, J. S., KIM, H. H., CHOI, J. Y., SUH, S. H. & BAEK, S. H. 2017. Investigation of the effects of miniscrew-assisted rapid palatal expansion on airflow in the upper airway of an adult patient with obstructive sleep apnea syndrome using computational fluid-structure interaction analysis. *Korean J Orthod*, 47, 353-364.
66. JIA, H., ZHUANG, L., ZHANG, N., BIAN, Y. & LI, S. 2021. Comparison of skeletal maxillary transverse deficiency treated by microimplant-assisted rapid palatal expansion and tooth-borne expansion during the post-pubertal growth spurt stage. *Angle Orthod*, 91, 36-45.
67. KANG, Q., CHA, C., HUANG, D., ZUO, S. & YAN, X. 2020. Evaluation of palatal support tissues for placement of orthodontic mini-implants in mouth breathers with high-narrow palates versus nose breathers with normal palates: a retrospective study. *Clin Oral Investig*, 24, 1259-1267.
68. KANOMI, R. 1997. Mini-implant for orthodontic anchorage. *J Clin Orthod*, 31, 763-7.
69. KAPETANOVIĆ, A., THEODOROU, C. I., BERGÉ, S. J., SCHOLS, J. & XI, T. 2021. Efficacy of Miniscrew-Assisted Rapid Palatal Expansion (MARPE) in late adolescents and adults: a systematic review and meta-analysis. *Eur J Orthod*, 43, 313-323.
70. KATALINIC, A., TRINAJSTIC ZRINSKI, M., ROKSANDIC VRANCIC, Z. & SPALJ, S. 2017. Influence of Manual Screwdriver Design in Combination With and Without Predrilling on Insertion Torque of Orthodontic Mini-Implants. *Implant Dent*, 26, 95-100.
71. KERNEN, F., KRAMER, J., WANNER, L., WISMEIJER, D., NELSON, K. & FLÜGGE, T. 2020. A review of virtual planning software for guided implant surgery - data import and visualization, drill guide design and manufacturing. *BMC Oral Health*, 20, 251.
72. KIM, Y. K., KIM, Y. J., YUN, P. Y. & KIM, J. W. 2009. Effects of the taper shape, dual-thread, and length on the mechanical properties of mini-implants. *Angle Orthod*, 79, 908-14.
73. KOUDSTAAL, M. J., SMEETS, J. B., KLEINRENSINK, G. J., SCHULTEN, A. J. & VAN DER WAL, K. G. 2009. Relapse and stability of surgically assisted rapid maxillary expansion: an anatomic biomechanical study. *J Oral Maxillofac Surg*, 67, 10-4.
74. KOVURU, V., AILENI, K. R., MALLEPALLY, J. P., KUMAR, K. S., SURSALA, S. & PRAMOD, V. 2023. Factorial analysis of variables affecting bone stress adjacent to mini-implants used for molar distalization by direct anchorage-A finite element study. *J Orthod Sci*, 12, 18.
75. LAGRAVÈRE, M. O., CAREY, J., HEO, G., TOOGOOD, R. W. & MAJOR, P. W. 2010. Transverse, vertical, and anteroposterior changes from bone-anchored maxillary expansion vs traditional rapid maxillary expansion: a randomized clinical trial. *Am J Orthod Dentofacial Orthop*, 137, 304.e1-12; discussion 304-5.

76. LEE, K. J., PARK, Y. C., PARK, J. Y. & HWANG, W. S. 2010. Miniscrew-assisted nonsurgical palatal expansion before orthognathic surgery for a patient with severe mandibular prognathism. *Am J Orthod Dentofacial Orthop*, 137, 830-9.
77. LI, L., ZHAI, M., WANG, M., CUI, S., CHENG, C., WANG, J. & WEI, F. 2023. Three-Dimensional Evaluation Effects of Microimplant-Assisted Rapid Palatal Expansion on the Upper Airway Volume: A Systematic Review and Meta-Analysis. *J Clin Med*, 12.
78. LIM, H. M., PARK, Y. C., LEE, K. J., KIM, K. H. & CHOI, Y. J. 2017. Stability of dental, alveolar, and skeletal changes after miniscrew-assisted rapid palatal expansion. *Korean J Orthod*, 47, 313-322.
79. LIN, J. H., LI, C., WONG, H., CHAMBERLAND, S., LE, A. D. & CHUNG, C. H. 2022. Asymmetric Maxillary Expansion Introduced by Surgically Assisted Rapid Palatal Expansion: A Systematic Review. *J Oral Maxillofac Surg*, 80, 1902-1911.
80. LIN, J. H., WANG, S., ABDULLAH, U. A., LE, A. D., CHUNG, C. H. & LI, C. 2023. Sagittal and Vertical Changes of the Maxilla after Surgically Assisted Rapid Palatal Expansion: A Systematic Review and Meta-Analysis. *J Clin Med*, 12.
81. LIN, L., AHN, H. W., KIM, S. J., MOON, S. C., KIM, S. H. & NELSON, G. 2015. Tooth-borne vs bone-borne rapid maxillary expanders in late adolescence. *Angle Orthod*, 85, 253-62.
82. LIOU, E. J. & TSAI, W. C. 2005. A new protocol for maxillary protraction in cleft patients: repetitive weekly protocol of alternate rapid maxillary expansions and constrictions. *Cleft Palate Craniofac J*, 42, 121-7.
83. LIU, S. Y., GUILLEMINAULT, C., HUON, L. K. & YOON, A. 2017. Distraction Osteogenesis Maxillary Expansion (DOME) for Adult Obstructive Sleep Apnea Patients with High Arched Palate. *Otolaryngol Head Neck Surg*, 157, 345-348.
84. LUDWIG, B., GLASL, B., BOWMAN, S. J., WILMES, B., KINZINGER, G. S. & LISSON, J. A. 2011. Anatomical guidelines for miniscrew insertion: palatal sites. *J Clin Orthod*, 45, 433-41; quiz 467.
85. MACGINNIS, M., CHU, H., YOUSSEF, G., WU, K. W., MACHADO, A. W. & MOON, W. 2014. The effects of micro-implant assisted rapid palatal expansion (MARPE) on the nasomaxillary complex--a finite element method (FEM) analysis. *Prog Orthod*, 15, 52.
86. MAINO, G. B., MAINO, G., CREMONINI, F. & LOMBARDO, L. 2023. Class III treatment with mini-implants anchorage in young adult patients: short and long-term results. *Dental Press J Orthod*, 28, e23spe2.
87. MECENAS, P., ESPINOSA, D. G., CARDOSO, P. C. & NORMANDO, D. 2020. Stainless steel or titanium mini-implants? *Angle Orthod*, 90, 587-597.
88. MEHTA, S., WANG, D., KUO, C. L., MU, J., VICH, M. L., ALLAREDDY, V., TADINADA, A. & YADAV, S. 2021. Long-term effects of mini-screw-assisted rapid palatal expansion on airway. *Angle Orthod*, 91, 195-205.
89. MEIRA, T. M., TANAKA, O. M., RONSANI, M. M., MARUO, I. T., GUARIZA-FILHO, O., CAMARGO, E. S. & MARUO, H. 2013. Insertion

- torque, pull-out strength and cortical bone thickness in contact with orthodontic mini-implants at different insertion angles. *Eur J Orthod*, 35, 766-71.
90. MENDES, M. B., MEDEIROS, R. C., LAURIA, A., MARCHIORI, É., SAWAZAKI, R., LOPES É, S. & MOREIRA, R. W. 2016. Mechanical and microstructural properties of fixation systems used in oral and maxillofacial surgery. *Oral Maxillofac Surg*, 20, 85-90.
 91. MÖHLHENRICH, S. C., HEUSSEN, N., ELVERS, D., STEINER, T., HÖLZLE, F. & MODABBER, A. 2015a. Compensating for poor primary implant stability in different bone densities by varying implant geometry: a laboratory study. *International Journal of Oral and Maxillofacial Surgery*, 44, 1514-1520.
 92. MÖHLHENRICH, S. C., HEUSSEN, N., MODABBER, A., BOCK, A., HÖLZLE, F., WILMES, B., DANESH, G. & SZALMA, J. 2020a. Influence of bone density, screw size and surgical procedure on orthodontic mini-implant placement - part B: implant stability. *Int J Oral Maxillofac Surg*.
 93. MÖHLHENRICH, S. C., KNIHA, K., PETERS, F., CHHATWANI, S., PRESCHER, A., HÖLZLE, F., MODABBER, A. & DANESH, G. 2020b. Anatomical assessment by cone beam computed tomography with the use of lateral cephalograms to analyse the vertical bone height of the anterior palate for orthodontic mini-implants. *Orthod Craniofac Res*.
 94. MÖHLHENRICH, S. C., MODABBER, A., STEINER, T., MITCHELL, D. A. & HÖLZLE, F. 2015b. Heat generation and drill wear during dental implant site preparation: systematic review. *Br J Oral Maxillofac Surg*, 53, 679-89.
 95. MOMMAERTS, M. Y. 1999. Transpalatal distraction as a method of maxillary expansion. *Br J Oral Maxillofac Surg*, 37, 268-72.
 96. NAVARRETE, V., ANGELES, R., VERNAL, R., VALDIVIA, E., VERGARA-BUENAVENTURA, A., MUNIZ, F. & CAFFERATA, E. A. 2024. Resistance to Torsion of Cement vs Screw-Retained Abutments Under a Tangential Load: A Pilot Study. *J Oral Implantol*, 50, 421-425.
 97. NAVEDA, R., DOS SANTOS, A. M., SEMINARIO, M. P., MIRANDA, F., JANSON, G. & GARIB, D. 2022. Midpalatal suture bone repair after miniscrew-assisted rapid palatal expansion in adults. *Prog Orthod*, 23, 35.
 98. NGAN, P., NGUYEN, U. K., NGUYEN, T., TREMONT, T. & MARTIN, C. 2018. Skeletal, Dentoalveolar, and Periodontal Changes of Skeletally Matured Patients with Maxillary Deficiency Treated with Microimplant-assisted Rapid Palatal Expansion Appliances: A Pilot Study.
 99. NIENKEMPER, M., PAULS, A., LUDWIG, B. & DRESCHER, D. 2015. Stability of paramedian inserted palatal mini-implants at the initial healing period: a controlled clinical study. *Clin Oral Implants Res*, 26, 870-875.
 100. NIENKEMPER, M., WILLMANN, J. H., BECKER, K. & DRESCHER, D. 2020. RFA measurements of survival midpalatal orthodontic mini-implants in comparison to initial healing period. *Prog Orthod*, 21, 5.
 101. NIENKEMPER, M., WILMES, B., PAULS, A. & DRESCHER, D. 2013a. Impact of mini-implant length on stability at the initial healing period: a controlled clinical study. *Head Face Med*, 9, 30.
 102. NIENKEMPER, M., WILMES, B., PAULS, A. & DRESCHER, D. 2013b. Maxillary protraction using a hybrid hyrax-facemask combination. *Prog Orthod*, 14, 5.

103. ODENRICK, L., LILJA, E. & LINDBÄCK, K. F. 1982. Root surface resorption in two cases of rapid maxillary expansion. *Br J Orthod*, 9, 37-40.
104. OLIVEIRA, C. B., AYUB, P., ANGELIERI, F., MURATA, W. H., SUZUKI, S. S., RAVELLI, D. B. & SANTOS-PINTO, A. 2021a. Evaluation of factors related to the success of miniscrew-assisted rapid palatal expansion. *Angle Orthod*, 91, 187-194.
105. OLIVEIRA, P. L. E., SOARES, K. E. M., ANDRADE, R. M., OLIVEIRA, G. C., PITHON, M. M., ARAÚJO, M. T. S. & SANT'ANNA, E. F. 2021b. Stress and displacement of mini-implants and appliance in Mini-implant Assisted Rapid Palatal Expansion: analysis by finite element method. *Dental Press J Orthod*, 26, e21203.
106. OTHMAN, A., ARNOLD, J., STRÖBELE, D. & VON SEE, C. 2020. A digitally designed and sinter laser-melted Hybrid Hyrax. *J Clin Orthod*, 54, 336-340.
107. PARK, J. J., PARK, Y. C., LEE, K. J., CHA, J. Y., TAHK, J. H. & CHOI, Y. J. 2017. Skeletal and dentoalveolar changes after miniscrew-assisted rapid palatal expansion in young adults: A cone-beam computed tomography study. *Korean J Orthod*, 47, 77-86.
108. PATIÑO, A. M. B., RODRIGUES, M. P., PESSOA, R. S., RUBINSKY, S. Y., KIM, K. B., SOARES, C. J. & ALMEIDA, G. A. 2024. Biomechanical behavior of three maxillary expanders in cleft lip and palate: a finite element study. *Braz Oral Res*, 38, e010.
109. PEREIRA FILHO, V. A., IAMASHITA, H. Y., MONNAZZI, M. S., GABRIELLI, M. F., VAZ, L. G. & PASSERI, L. A. 2013. In vitro biomechanical evaluation of sagittal split osteotomy fixation with a specifically designed miniplate. *Int J Oral Maxillofac Surg*, 42, 316-20.
110. PICKARD, M. B., DECHOW, P., ROSSOUW, P. E. & BUSCHANG, P. H. 2010. Effects of miniscrew orientation on implant stability and resistance to failure. *Am J Orthod Dentofacial Orthop*, 137, 91-9.
111. PIMENTEL, A. C., MANZI, M. R., PRADO BARBOSA, A. J., COTRIM-FERREIRA, F. A., GUEDES CARVALHO, P. E., DE LIMA, G. F. & ZINDEL DEBONI, M. C. 2016. Mini-Implant Screws for Bone-Borne Anchorage: A Biomechanical In Vitro Study Comparing Three Diameters. *Int J Oral Maxillofac Implants*, 31, 1072-6.
112. PITHON, M. M., FIGUEIREDO, D. S. & OLIVEIRA, D. D. 2013. Mechanical evaluation of orthodontic mini-implants of different lengths. *J Oral Maxillofac Surg*, 71, 479-86.
113. PRÉVÉ, S. & GARCÍA ALCÁZAR, B. 2022. Interest of miniscrew-assisted rapid palatal expansion on the upper airway in growing patients: A systematic review. *Int Orthod*, 20, 100657.
114. RACHMIEL, A., TURGEMAN, S., SHILO, D., EMODI, O. & AIZENBUD, D. 2020. Surgically Assisted Rapid Palatal Expansion to Correct Maxillary Transverse Deficiency. *Ann Maxillofac Surg*, 10, 136-141.
115. REN, Y. 2009. Mini-implants for direct or indirect orthodontic anchorage. *Evid Based Dent*, 10, 113.
116. RITTO, A. K. 2004. Micro implants in orthodontics. *Int J Orthod Milwaukee*, 15, 22-4.

117. RODRIGUES, S. A., PRESOTTO, A. G. C., BARÃO, V. A. R., CONSANI, R. L. X., NÓBILO, M. A. A. & MESQUITA, M. F. 2017. The role of welding techniques in the biomechanical behavior of implant-supported prostheses. *Mater Sci Eng C Mater Biol Appl*, 78, 435-442.
118. SADR HAGHIGHI, A. H., POUYAFAR, V., NAVID, A., ESKANDARINEZHAD, M. & ABDOLLAHZADEH BAGHAEI, T. 2019. Investigation of the optimal design of orthodontic mini-implants based on the primary stability: A finite element analysis. *J Dent Res Dent Clin Dent Prospects*, 13, 85-89.
119. SAKAMAKI, T., WATANABE, K., IWASA, A., DEGUCHI, T., HORIUCHI, S. & TANAKA, E. 2022. Thread shape, cortical bone thickness, and magnitude and distribution of stress caused by the loading of orthodontic miniscrews: finite element analysis. *Sci Rep*, 12, 12367.
120. SANA, S., REDDY, R., TALAPANENI, A. K., HUSSAIN, A., BANGI, S. L. & FATIMA, A. 2020. Evaluation of stability of three different mini-implants, based on thread shape factor and numerical analysis of stress around mini-implants with different insertion angle, with relation to en-masse retraction force. *Dental Press J Orthod*, 25, 59-68.
121. SFONDRINI, M. F., GANDINI, P., ALCOZER, R., VALLITTU, P. K. & SCRIBANTE, A. 2018. Failure load and stress analysis of orthodontic miniscrews with different transmucosal collar diameter. *J Mech Behav Biomed Mater*, 87, 132-137.
122. SHETTY, V., CARIDAD, J. M., CAPUTO, A. A. & CHACONAS, S. J. 1994. Biomechanical rationale for surgical-orthodontic expansion of the adult maxilla. *J Oral Maxillofac Surg*, 52, 742-9; discussion 750-1.
123. SHIN, Y. S., AHN, H. W., PARK, Y. G., KIM, S. H., CHUNG, K. R., CHO, I. S. & NELSON, G. 2012. Effects of predrilling on the osseointegration potential of mini-implants. *Angle Orthod*, 82, 1008-13.
124. SILVA, I., MIRANDA, F., BASTOS, J. & GARIB, D. 2024. Comparison of alveolar bone morphology after expansion with hybrid and conventional Hyrax expanders. *Angle Orthod*, 94, 414-420.
125. SONG, S. Y., LEE, J. Y. & SHIN, S. W. 2017. Effect of Implant Diameter on Fatigue Strength. *Implant Dent*, 26, 59-65.
126. SU, Y. Y., WILMES, B., HÖNSCHEID, R. & DRESCHER, D. 2009. Comparison of self-tapping and self-drilling orthodontic mini-implants: an animal study of insertion torque and displacement under lateral loading. *Int J Oral Maxillofac Implants*, 24, 404-11.
127. TANAKA, O. & MOTA-JÚNIOR, S. L. 2023. MARPE as an adjunct to orthodontic treatment. *Dental Press J Orthod*, 27, e22bbo6.
128. TATLI, U., ALRAAWI, M. & TOROGLU, M. S. 2019. Effects of size and insertion angle of orthodontic mini-implants on skeletal anchorage. *Am J Orthod Dentofacial Orthop*, 156, 220-228.
129. TOYOSHIMA, Y. & WAKABAYASHI, N. 2015. Load limit of mini-implants with reduced abutment height based on fatigue fracture resistance: experimental and finite element study. *Int J Oral Maxillofac Implants*, 30, e10-6.
130. UDOMSAWAT, C., RUNGSIYAKULL, P., RUNGSIYAKULL, C. & KHONGKHUNTHIAN, P. 2019. Comparative study of stress characteristics in

- surrounding bone during insertion of dental implants of three different thread designs: A three-dimensional dynamic finite element study. *Clin Exp Dent Res*, 5, 26-37.
131. UMALKAR, S. S., JADHAV, V. V., PAUL, P. & RECHE, A. 2022. Modern Anchorage Systems in Orthodontics. *Cureus*, 14, e31476.
 132. VILLA-OBANDO, Y. A., CORREA-OSORIO, S. M., CASTRILLON-MARIN, R. A., VIVARES-BUILES, A. M. & ARDILA, C. M. 2024. Effect of Anchorage Modifications on the Efficacy of Miniscrew-Assisted Rapid Palatal Expansion: A Systematic Review and Meta-Analysis. *Cureus*, 16, e72008.
 133. WALTER, A., DE LA IGLESIA, F., WINSAUER, H., PLODER, O., WENDL, B. & PUIGDOLLERS PEREZ, A. 2023. Evaluation of expansion forces of five pure bone-borne maxillary expanders designs anchored with orthodontic mini-implants: An in vitro study. *J Orthod*, 14653125231152502.
 134. WALTER, A., WINSAUER, H., MARCÉ-NOGUÉ, J., MOJAL, S. & PUIGDOLLERS, A. 2013. Design characteristics, primary stability and risk of fracture of orthodontic mini-implants: pilot scan electron microscope and mechanical studies. *Med Oral Patol Oral Cir Bucal*, 18, e804-10.
 135. WILMES, B. 2022. „Appliance First“ or „Bone First“ for miniscrew assisted rapid palatal expansion“. *APOS Trends in Orthodontics*, 12, 3-6.
 136. WILMES, B., BECKER, K., WILLMANN, J., TARRAF, N. E. & DRESCHER, D. 2022a. Maxillary expansion and protraction using mini-implants and the benefit direct mechanism. *J Clin Orthod*, 56, 708-715.
 137. WILMES, B. & DRESCHER, D. 2009. Impact of insertion depth and predrilling diameter on primary stability of orthodontic mini-implants. *Angle Orthod*, 79, 609-14.
 138. WILMES, B. & DRESCHER, D. 2011. Impact of bone quality, implant type, and implantation site preparation on insertion torques of mini-implants used for orthodontic anchorage. *Int J Oral Maxillofac Surg*, 40, 697-703.
 139. WILMES, B., LUDWIG, B., KATYAL, V., NIENKEMPER, M., REIN, A. & DRESCHER, D. 2014a. The Hybrid Hyrax Distalizer, a new all-in-one appliance for rapid palatal expansion, early class III treatment and upper molar distalization. *J Orthod*, 41 Suppl 1, S47-53.
 140. WILMES, B., LUDWIG, B., VASUDAVAN, S., NIENKEMPER, M. & DRESCHER, D. 2016. The T-Zone: Median vs. Paramedian Insertion of Palatal Mini-Implants. *J Clin Orthod*, 50, 543-551.
 141. WILMES, B., NGAN, P., LIOU, E. J., FRANCHI, L. & DRESCHER, D. 2014b. Early class III facemask treatment with the hybrid hyrax and Alt-RAMEC protocol. *J Clin Orthod*, 48, 84-93.
 142. WILMES, B., NIENKEMPER, M. & DRESCHER, D. 2010. Application and effectiveness of a mini-implant- and tooth-borne rapid palatal expansion device: the hybrid hyrax. *World J Orthod*, 11, 323-30.
 143. WILMES, B., OTTENSTREUER, S., SU, Y. Y. & DRESCHER, D. 2008a. Impact of implant design on primary stability of orthodontic mini-implants. *J Orofac Orthop*, 69, 42-50.
 144. WILMES, B., RADEMACHER, C., OLTHOFF, G. & DRESCHER, D. 2006. Parameters affecting primary stability of orthodontic mini-implants. *J Orofac Orthop*, 67, 162-74.

145. WILMES, B., SU, Y. Y. & DRESCHER, D. 2008b. Insertion angle impact on primary stability of orthodontic mini-implants. *Angle Orthod*, 78, 1065-70.
146. WILMES, B., TARRAF, N. & DRESCHER, D. 2021. Treatment of maxillary transversal deficiency by using a mini-implant-borne rapid maxillary expander and aligners in combination. *Am J Orthod Dentofacial Orthop*, 160, 147-154.
147. WILMES, B., TARRAF, N. E., DE GABRIELE, R., DALLATANA, G. & DRESCHER, D. 2022b. Procedure using CAD/CAM-manufactured insertion guides for purely mini-implant-borne rapid maxillary expanders. *J Orofac Orthop*, 83, 277-284.
148. YADAV, S., UPADHYAY, M., LIU, S., ROBERTS, E., NEACE, W. P. & NANDA, R. 2012. Microdamage of the cortical bone during mini-implant insertion with self-drilling and self-tapping techniques: a randomized controlled trial. *Am J Orthod Dentofacial Orthop*, 141, 538-46.
149. YI, F., LIU, S., LEI, L., LIU, O., ZHANG, L., PENG, Q. & LU, Y. 2020. Changes of the upper airway and bone in microimplant-assisted rapid palatal expansion: A cone-beam computed tomography (CBCT) study. *J Xray Sci Technol*, 28, 271-283.
150. YILMAZ, A., ARMAN-ÖZÇİRPİCİ, A., ERKEN, S. & POLAT-ÖZSOY, Ö. 2015. Comparison of short-term effects of mini-implant-supported maxillary expansion appliance with two conventional expansion protocols. *Eur J Orthod*, 37, 556-64.
151. ZENG, W., YAN, S., YI, Y., CHEN, H., SUN, T., ZHANG, Y. & ZHANG, J. 2023. Long-term efficacy and stability of miniscrew-assisted rapid palatal expansion in mid to late adolescents and adults: a systematic review and meta-analysis. *BMC Oral Health*, 23, 829.
152. ZIMRING, J. F. & ISAACSON, R. J. 1965. FORCES PRODUCED BY RAPID MAXILLARY EXPANSION. 3. FORCES PRESENT DURING RETENTION. *Angle Orthod*, 35, 178-86.

8 Appendix

8.1 Figures

Fig. 1: Material diagram.....	9
Fig. 2: Clinical example	10
Fig. 3: Clinical example	11
Fig. 4: Two different types of mini-implants and the BMX expansion screw.....	12
Fig. 5: Benefit direct mini-implant: The polyaxial thread	13
Fig. 6: Example of DIRECT insertion in different angles	15
Fig. 7: Computer-assisted fabrication of the insertion guides for predrilling and insertion in Blender	16
Fig. 8: Double guides with Mini-Raft support structures	16
Fig. 9: Double guides position before starting the printing process	17
Fig 10: Summary of the preparation of the ideal position for the printing process in Preform	17
Fig. 11: CAD/CAM production steps of the double guides.....	18
Fig. 12: Benefit standard 0° mini-implant placement.....	20
Fig. 13: Benefit direct 0° mini-implant placement	20
Fig. 14: Benefit direct 5° mini-implant placement	21
Fig. 15: Benefit direct 10° mini-implant placement	21
Fig. 16: Benefit direct 15° mini-implant placement	22
Fig. 17: Schematic illustration of the experimental set-up	23
Fig. 18: Picture of the experimental setup	24
Fig. 19: Force-displacement graph comparing benefit 0°, direct 0°, direct 5°, direct 10° and direct 15°	24
Fig. 20: Maximum forces of all groups.....	26
Fig. 21: Deformation limits of all groups	27

8.2 Tables

Tab. 1: Summary of the included mini-implants	13
Tab. 2: Solid rigid polyurethane foam properties	19
Tab. 3: Test of normality	25
Tab. 4: Descriptive statistics of the maximum force, deformation limit, and activation of all groups	27
Tab. 5: Estimated marginal means comparing all groups.....	29
Tab. 6: Estimated marginal means comparing control group and Direct group.....	30
Tab. 7: Box's Test.....	31
Tab. 8: Levene's test.....	32
Tab. 9: Multivariate ANOVA	32
Tab. 10: ANOVA.....	32
Tab. 11: ANOVA measures of association.....	33
Tab. 12: Bonferroni post hoc test comparing all groups for maximum force and deformation limit	34
Tab. 13: Non-parametric test summary for the activation in mm between the control group and Direct groups	36
Tab. 14: Kruskal-Wallis Test for the activation across the control group and all Direct groups	37
Tab. 15: Kruskal-Wallis Test for activation across the control group and the angle- altered Direct groups 1-4	37
Tab. 16: Post hoc Dunn-Bonferroni test after Kruskal-Wallis test.....	38

Acknowledgement

First and foremost, I would like to express my sincere gratitude to my doctoral supervisor, Prof. Dr. Dieter Drescher, for entrusting me with this research matter. As my orthodontist, he not only inspired me to pursue a career in dentistry but also guided me with invaluable expertise, continuous encouragement, and support throughout this study. I am proud to have been able to follow his academic path up to the doctoral level under his personal supervision.

I would like to thank Sawbone and Burster, as well as PSM Medical Solutions, for generously providing the resources essential for conducting this study.

Special thanks go to Mr. Bernd Münstermann, and the precision mechanic and technical assistant, whose technical support and assistance were instrumental in the successful realization of the experimental setup.

I am grateful to my colleagues in dentistry for their insightful suggestions and enriched discussions, which added meaningful perspectives to my work.

A very special thanks goes to my sister Patricia, who was always there to listen patiently and wholeheartedly. Her calm presence and constant emotional support were a source of strength in times of doubt and challenge.

I am deeply grateful for the love and belief of my partner. He has been my anchor in times of stress, my source of joy, and the steady hand that carried me through the most demanding phases of this journey. His support has meant more than words can express.

Above all, I wish to extend my sincere gratitude to my grandmother Lucie, who would have been immensely proud to witness its completion. Her memory remains a powerful source of inspiration for my life achievements.

Finally, I wish to dedicate this work to my parents, Dres. med. Danuta and Gotthard Grützner, whose unwavering encouragement and confidence in my abilities have been instrumental in initiating and successfully concluding this academic path. They have fostered my sustained interest in medicine and research and made my education in dentistry and medicine possible. Their love remains my most profound source of motivation.